This information is current as of November 26, 2013.

Expression of CXCR3 on Specific T Cells Is Essential for Homing to the Prostate Gland in an Experimental Model of Chronic Prostatitis/Chronic Pelvic Pain Syndrome

Maria L. Breser, Ruben D. Motrich, Leonardo R. Sanchez, Juan P. Mackern-Oberti and Virginia E. Rivero

J Immunol 2013; 190:3121-3133; Prepublished online 1 March 2013;
doi: 10.4049/jimmunol.1202482
http://www.jimmunol.org/content/190/7/3121

The Journal of Immunology is published twice each month by
The American Association of Immunologists, Inc.,
9650 Rockville Pike, Bethesda, MD 20814-3994.

Print ISSN: 0022-1767 Online ISSN: 1550-6606.

Expression of CXCR3 on Specific T Cells Is Essential for Homing to the Prostate Gland in an Experimental Model of Chronic Prostatitis/Chronic Pelvic Pain Syndrome

Maria L. Breser, Ruben D. Motrich, Leonardo R. Sanchez, Juan P. Mackern-Oberti, and Virginia E. Rivero

Experimental autoimmune prostatitis (EAP) is considered a valid model for the human disease chronic prostatitis/chronic pelvic pain syndrome. In this report, we analyzed phenotypic characteristics of T cells that gain access to the prostate and induce leukocyte recruitment in mice with different susceptibility to EAP. After EAP induction, NOD mice developed a specific cellular response characterized by a mixed Th1/Th17 pattern with specific T cells mainly expressing CXCR3 that infiltrated and damaged the prostate. In contrast, BALB/c mice, as well as NOD-IFN-$\gamma^{-/-}$, exhibited only Th17 cells mainly expressing CCR6 that were not capable of infiltrating the prostate gland. Adoptive transfer experiments of T cells from NOD or NOD–IFN-$\gamma^{-/-}$ mice to NOD-SCID recipients showed that only T cells from NOD mice successfully infiltrated the prostate. However, after "in vitro" or "in vivo" treatment with rIFN-γ, T cells from NOD–IFN-$\gamma^{-/-}$ mice became capable of homing to the prostate and induced leukocyte recruitment. Chemokine levels in prostate tissue from NOD mice showed increased expression levels of CXCR3 ligands. Additional experiments using adoptive transfer of sorted CXCR3$^+$CD3$^+$ T cells or administrating a CXCR3 antagonist treatment confirmed these previous results. Altogether, our results demonstrate that the expression of CXCR3 on effector T cells is essential for their homing to the prostate gland in EAP. CXCR3 emerges as a potential therapeutic target to control chronic prostatitis/chronic pelvic pain syndrome. ***The Journal of Immunology*****, 2013, 190: 3121–3133.**

Prostatitis is the most common urologic diagnosis in men aged <50 y and the third most common urologic diagnosis in men aged >50 y after benign prostate hyperplasia and prostate cancer (1, 2). The National Institutes of Health (NIH) consensus definition and classification identifies four categories of prostatitis (3). Categories I and II have bacterial causes, whereas III and IV have traditionally been considered to have nonbacterial cause (3, 4). Category III prostatitis or chronic pelvic pain syndrome (CPPS) is the most common type of prostatitis observed in medical practice, representing 90% of cases. CPPS is a poorly understood entity characterized by pelvic or perineal pain, irritative voiding symptoms, and sexual dysfunction, and, from a clinical point of view, is truly lacking a cause that would allow a more rational-driven therapy (1–4).

Centro de Investigaciones en Bioquímica Clínica e Inmunología, Departamento de Bioquímica Clínica, Facultad de Ciencias Químicas, Universidad Nacional de Córdoba, Córdoba, 5016 Argentina

Received for publication September 6, 2012. Accepted for publication January 24, 2013.

This work was supported by Secretaria de Ciencia y Técnica de la Universidad Nacional de Cordoba and Agencia Nacional de Promoción Científica y Tecnológica Grants PICT 2005-38069 and PICT 2008-1639. The TAK-779 reagent was obtained through the AIDS Research and Reference Reagent Program, Division of Acquired Immunodeficiency Syndrome, National Institute of Allergy and Infectious Diseases, National Institutes of Health (Germantown, MD).

Address correspondence and reprint requests to Dr. Virginia Rivero, Centro de Investigaciones en Bioquimica Clinica e Inmunologia (CIBICI-CONICET), Inmunología, Departamento de Bioquímica Clínica, Facultad de Ciencias Químicas, Universidad Nacional de Córdoba, Haya de la Torre y Medina Allende, Ciudad Universitaria, Córdoba, 5016 Argentina. E-mail address: vrivero@fcq.unc.edu.ar

The online version of this article contains supplemental material.

Abbreviations used in this article: CP, chronic prostatitis; CPPS, chronic pelvic pain syndrome; EAP, experimental autoimmune prostatitis; LN, lymph node; PAg, mixture of prostate Ag; PSBP, prostate steroid-binding protein.

Some researchers, including us, have postulated an autoimmune cause for chronic prostatitis (CP)/CPPS (4). Evidence of an autoimmune basis in CP/CPPS comes from a number of studies in humans. Self-reactivity of T cells from men with CP/CPPS to seminal plasma proteins and normal prostatic proteins, such as prostate-specific Ag and prostatic acid phosphatase, has already been reported (5–8). In addition, increased levels of TNF-α, IL-1β, and IFN-γ in seminal fluid of men with CP/CPPS (9–11), the presence of IFN-γ–secreting lymphocytes specific to prostate Ags (5), and the presence of prostatic intra-acinar T cell–rich infiltrates in CP/CPPS patients (12) have also been described.

In addition, substantial evidence for an autoimmune cause in CP/CPPS comes from animal models of autoimmune prostatitis (13). Our laboratory has pioneered the development of animal models of experimental autoimmune prostatitis (EAP), which is achieved by immunization of animals with prostate Ags plus adjuvant. These models show almost all previously mentioned characteristics of human disease: the presence of IFN-γ–secreting lymphocytes specific to prostate Ags, increased levels of cytokines in semen, pelvic pain, inflammation, and the type of infiltration and histological lesions seen in the target organ (13–16). Studies focused on differential susceptibility to the development of EAP have shown that NOD, C57BL/6, SJL, A/J, and BALB/c mice exhibited different severity of prostatic inflammation after EAP induction, with NOD and BALB/c mice the most susceptible and the most resistant strains, respectively (4, 13, 17). NOD mice develop severe inflammation in the prostate, accompanied by specific T cell–mediated responses that could be assessed by in vitro–specific proliferation and IFN-γ production, but not IL-4 secretion (14, 18). A crucial role of IFN-γ in EAP has been shown because the absence of IFN-γ or transcription factors involved in the IFN-γ signaling cascade, such as IRF-1 and STAT-1, made mice resistant to EAP induction (14, 19). Recently, IL-17 produced by Th17 cells has been recognized as critical for the development

of autoimmune diseases such as rheumatoid arthritis, EAE, and others (20). Currently, Th17 cells have been identified as major players in many autoimmune processes, but their role in EAP is still uncertain.

In experimental models of autoimmunity, pathogenic effectors Th1 and Th17 cells once induced in periphery must traffic to their target organs. This traffic is associated with the expression of specific chemokine receptors and also to the induction of appropriate chemokines in the target organ (21). $CD3^+$ T cell–driven inflammation is characterized by the predominant type of cytokines secreted by infiltrating T cells. In turn, these cytokines induce specific subsets of IFN-γ–inducible chemokines, IL-4– and IL-13–inducible chemokines, or IL-17–inducible chemokines at the site of inflammation (22). Then these chemokines induce the recruitment of T cells and other immune cells that express the specific cognate receptors for these inflammatory chemokines (22).

The mechanisms that regulate lymphocyte recruitment, positioning, and persistence within the prostate are currently unknown, but as for other tissue-homing mechanisms, chemokines and their receptors are likely to play an important role (23). In this work, we show that after EAP induction in mice with different susceptibility to autoimmunity, autoreactive Th1/Th17 or Th17 cells are induced, express different chemokine receptor patterns, and thus different capabilities of infiltrating the prostate gland. Although both specific cell subsets are induced, only Th1 cells, but not Th17 cells, seem to be indispensable in the pathogenesis of autoimmune prostatitis. Our results demonstrate that the expression of CXCR3 on effectors T cells is associated with their homing to the prostate gland in EAP.

Materials and Methods

Mice and Ags

Six- to 8-wk-old NOD/LtJ (NOD/ShiLtJ) and BALB/c mice were purchased from The Jackson Laboratory (Bar Harbor, ME). NOD-SCID (NOD.CB17-Prkdc^{scid}/J) and NOD–IFN-$\gamma^{-/-}$ (NOD.129S7(B6)-IFN-γ^{tm1Ts}) mice were kindly provided by Dr. Diane Mathis and Christophe Benoist (The Jackson Laboratory). All the animals were housed and bred in the specific pathogen-free research animal facility of our institution. A mixture of prostate Ags (PAg) and prostate steroid-binding protein (PSBP) were prepared as described previously (15). The purity of the PSBP preparation was >95% evaluated by Western blotting and was LPS free tested by Gel clot 0.03 endotoxin units/ml sensitivity (Charles River, Laboratories International, Wilmington, NY).

Antibodies

Commercially available Abs used in different experiments performed and their respective manufacturer were as follows: anti-CD4 (RM4-5), anti-CD11b (M1/70), anti-CD3 (145-2C11), anti-GR1 (RB6-8C5), anti–IFN-γ (XMG1.2), anti–IL-17A (TC11-18H10), anti–IL-10 (JES5-16E3), and IgG1 isotype controls were purchased from BD Pharmingen (San Diego, CA). Anti-CD8a (53-6.7), anti–IL-17A (eBIO17B7), anti–IL-10 (JES5-16E3), and anti-CD45 (30-F11) were purchased from eBioscience (San Diego, CA). Anti-CD45 (30-F11), anti-CD11b (M1/70), anti-Ly6G (1A8), anti-CCR6 (29-2L17), anti-CXCR3 (CXCR3-173), anti-CCR4 (2G12), anti-CCR5 (HM-CCR5), and anti-CCR3 (TG14/CCR3) were purchased from BioLegend (San Diego, CA). Abs were allophycocyanin, FITC, PE, PerCP-Cy5.5, Alexa Fluor 647, or PE-Cy7 conjugated and were properly combined.

EAP induction and histological score

Six- to 8-wk-old male NOD, NOD–IFN-$\gamma^{-/-}$, and BALB/c mice were included in the study. All the experimental protocols were reviewed and approved by our Institutional Review Board. Mouse experimental protocols were approved by the Institutional Ethical and Animal Care and Use Committee. Mice were s.c. immunized in the hind footpad and in the base of the tail with PAg (300 μg/mouse; PAg group) or saline solution (control group) emulsified in CFA (Sigma-Aldrich, St. Louis, MO) in a total volume of 150 μl/mouse. Other groups of mice were immunized with OVA (grade V; Sigma-Aldrich) emulsified in CFA (300 μg/mouse; OVA group). Mice received immunizations at days 0 and 15, and then were sacrificed at day 24 of the experimental schedule. Severity of EAP was assessed by determining the histological score, which was analyzed in a double-blind manner and computed for individual glands by summing the grade of each section and dividing by the total number of sections examined. The degree of inflammation was assessed using a score of 0–3 (15): 0, no inflammation; 1, mild, but definite perivascular cuffing with mononuclear cells; 2, moderate perivascular cuffing with mononuclear cells; 3, marked perivascular cuffing, hemorrhage, and numerous mononuclear cells in the parenchyma, in sections that were processed by conventional H&E staining.

Immunohistochemistry assays

Formalin-fixed and paraffin-embedded prostate sections were dewaxed in xylene, rehydrated, treated with Target Retrieval Solution (Dako Cytomation, Glostrup, Denmark) at 95°C for 30 min, and blocked with FC blocking solution (BD Pharmingen). Endogenous peroxidase activity was blocked with blocking buffer (Dako Cytomation). Then slides were incubated overnight at 4°C in blocking buffer containing rabbit anti-CD45 (clone 30-F11) Abs. Slides were washed four times in 10 mM PBS, 0.1% Tween 20, and incubated with anti-rabbit HRP (BD Pharmingen) secondary Abs for 2 h at room temperature. Colorimetric detection was performed by using Detection Kit (Becton Dickinson [BD] Bioscience) and counterstained with hematoxylin.

Cell culture

Single mononuclear cell suspensions were prepared in HBSS (Sigma-Aldrich) from spleen and draining lymph nodes (LNs) of individual mice by Histopaque centrifugation gradients. Live cells were counted by trypan blue exclusion, resuspended in RPMI 1640-GlutaMAX (Life Technologies, Carlsbad, CA), medium supplemented with 0.1% gentamicin (50 mg/ml), 1% penicillin/streptomycin (Life Technologies), 50 mM 2-ME (Life Technologies), and 10% FCS (Life Technologies), and cultured in the presence of PSBP (20 μg/ml) or medium alone. In some experiments, cells were cultured in the presence of OVA (20 μg/ml). All cell combinations were set up in triplicate. Plates were incubated for 72 h at 37°C in a water-saturated 5% CO_2 atmosphere. After that, cells were processed for surface or intracellular cytokine staining and analyzed by FACS. Supernatants were frozen at −80°C for cytokine determinations.

Cytokine quantitation assays

The measurement of IL-10, IL-17, and IFN-γ was performed by the use of ELISA kits (eBioscience and BD Biosciences) following manufacturer's instructions.

FACS analysis

Cells were in vitro stimulated with PSBP or OVA; then staining for cell-surface markers and intracellular cytokines was performed. In other experiments, after in vitro stimulation with PSBP or OVA for 72 h, cells were incubated for 5 h with PMA (10 ng/ml) and ionomycin (1 μg/ml) from Sigma-Aldrich. Brefeldin A (10 μg/ml; Sigma-Aldrich) was added in the last 4 h of culture. Cell-surface staining of different molecules was performed followed by intracellular staining of different cytokines using the CytoFix/CytoPerm kit (BD Biosciences) according to the manufacturer's instructions. Cells were acquired on a FACSCanto II (BD Biosciences) flow cytometer and analyzed using FlowJo software (Tree Star, Ashland, OR).

Analysis of prostate- and pancreas-infiltrating leukocytes

Freshly harvested prostate or pancreatic tissue were mechanically disrupted and enzymatically digested in RPMI 1640 medium containing 1 mg/ml collagenase D (Roche, Basilea, Switzerland) and DNase I (Sigma-Aldrich) for 45 min at 37°C. After digestion, suspensions were filtered through 75- and 40-μm cell strainers (BD Biosciences) and single-cell suspensions were washed twice in RPMI 1640 with 10% FBS, 2 mM EDTA, and 50 mM 2-ME supplemented medium. Live lymphocyte counts were deduced from the acquisition of a fixed number of 10-μm latex beads (Beckman Coulter, Brea, CA) mixed with a known volume of unstained cell suspension in propidium iodide. Analyses were performed on a FACSCanto II using DIVA software (BD Biosciences), allowing the exclusion of dead cells (propidium iodide positive) inside the indicated gates. After that, cells were stained with different Abs for FACS analysis. Cells were acquired using a FACSCanto II, and data were analyzed using FlowJo software (Tree Star).

Analysis of chemokine and cytokine expression in prostatic tissue

Prostates from control and immunized animals were obtained and excised at day 24 of the experimental schedule, and the expression levels of a panel of 96 cytokines and chemokines in tissue samples were measured using a mouse cytokine/chemokine array kit (Ray Biotech, Norcross, GA) following manufacturer's instructions and software.

Cell adoptive transfer experiments

Single mononuclear cell suspensions were prepared in HBSS (Sigma-Aldrich) from spleen and draining LNs of individual mice by Histopaque centrifugation gradients. Mononuclear cells were in vitro cultured in the presence of PSBP (20 μg/ml) for 72 h. In some experiments, mouse rIFN-γ (PeproTech, Mexico DF, Mexico) was also added to the culture medium in a final concentration of 1000 pg/ml. After that, cells were stained with anti-CD3 or anti-CD3 plus anti-CXCR3 mAbs and sorted using a FACSAria II cell sorter (BD Biosciences). Purity of >98% was achieved. Cells were resuspended at a density of 1×10^6 $CD3^+$ T cells in 100 μl sterile pyrogen-free PBS were injected into the retro-orbital plexus from NOD-SCID recipient mice (6–8 wk old). NOD-SCID recipients were euthanized at days 15 and 30 after cell transfer. Spleen, nondraining LNs, draining LNs, or prostate cells were stained and analyzed by FACS.

In vivo treatment with the chemokine receptor antagonist TAK-779

TAK-779 dose regimen and treatment were performed as previously described to block CXCR3 (24, 25). NOD-SCID mice recipients that were adoptively transferred with $CD3^+$ T cells were i.p. treated with TAK-779 (obtained from the NIH AIDS Research and Reference Reagent Program) or vehicle. Every animal received a treatment consisting in single injections of TAK-779 (150 μg dissolved in 150 μl pyrogen-free bidistilled water) or vehicle every 2 d after adoptive transfer and until day 30 after transfer. Every mouse received a total of 15 injections.

In vivo treatment with rIFN-γ

In some experiments, NOD–IFN-$\gamma^{-/-}$ were i.p. treated with 10^4 U/day rIFN-γ resuspended in 100 μl of 0.1% BSA/PBS. Injections were performed on days 16, 18, 20, and 22 of the experimental schedule.

Statistics

Statistical analysis was performed using one-way or two-way ANOVA with Bonferroni post hoc test analysis. Mean ± SEM are represented in the graphs. Statistical tests were performed using the GraphPad Prism 5.0 software. The p values ($^*p < 0.05$, $^{**}p < 0.01$, $^{***}p < 0.001$) were considered significant in all analyses.

Results

Specific Th1 and Th17 cells are induced in mice with differential susceptibility to EAP induction

Previously, we reported that Th1 cells play a crucial role in EAP (19). However, no conclusive evidence about the role of Th17 cells in autoimmune prostatitis has been reported to date. Considering that, we analyzed the induction of specific Th17 cells after immunization of NOD mice (highly susceptible) and BALB/c mice (resistant) with PAg. T cell–mediated response, assessed by in vitro release of cytokines after stimulation with the major autoantigen PSBP, showed a specific response characterized by high levels of IFN-γ and IL-17 secretion that could be detected in spleen and draining LNs from NOD mice (Fig. 1A). In contrast, very low levels of IFN-γ, but comparable levels of IL-17, were detected when assessing spleen and draining LN cells from BALB/c mice. Regarding PSBP-specific IL-10 secretion, comparable levels were shown in draining LN cells from NOD and BALB/c mice, although a significant increase was observed when spleen T cells from BALB/c mice were assayed (Fig. 1A). Because cytokine double-positive $CD4^+$ T cells exerting effector or regulatory functions have been reported (26), we next searched for the presence of $CD4^+$IFN-γ^+IL-17^+ and $CD4^+$IL-10^+IL-17^+ T cells after EAP induction. As shown in Fig. 1B and 1C, significantly higher frequencies of $CD4^+$IFN-γ^+ simple positive T cells and also $CD4^+$IL-17^+ T cells were present in NOD mice. On the contrary, BALB/c mice showed a significantly higher frequency of $CD4^+$IL-10^+ simple positive T cells and comparable levels of $CD4^+$IL-17^+ T cells after in vitro stimulation with PSBP when compared with the ones observed in NOD mice (Fig. 1B, 1C). Nevertheless, no presence of $CD4^+$IL-10^+IL-17^+ T cells was observed in both mouse strains (Fig. 1B).

Immunohistochemistry assays revealed a marked $CD45^+$ cell infiltration in different parts of the prostate gland of immunized NOD mice, whereas almost no infiltration was detected in prostate sections from immunized BALB/c mice (Fig. 1D). Flow cytometry assays revealed that $CD45^+$ cell infiltration in the prostate of immunized NOD mice was mainly composed of $CD3^+$ cells (Fig. 1E). Both $CD4^+$ and $CD8^+$ T lymphocytes were present in the infiltrating cell populations (data not shown). On the contrary, prostates from BALB/c mice showed a subtle increase in $CD45^+$ cell infiltration, mainly composed of $F480^+$ cells (Fig. 1E).

To evaluate the specificity of the response, we performed experiments in which NOD and BALB/c mice were immunized with PAg or a nonrelated Ag, like OVA, emulsified in CFA. After that, assays of Ag-specific cytokine responses were performed. Lymphocytes from immunized mice were stimulated in vitro with PSBP or OVA alone or PSBP/OVA plus PMA/ionomycin. As shown in Supplemental Fig. 1A, IFN-γ and IL-17 secretion could be detected in culture supernatants only when the corresponding Ag was added for in vitro stimulation. In addition, IFN-γ^+CD4^+ or IL-17^+CD4^+ cells were present when T cells were in vitro stimulated with the corresponding immunizing Ag alone (Supplemental Fig. 1B). When the assay was performed without PMA/ionomycin, values were low but still positive for the corresponding Ag only. Moreover, when the assay was performed in the presence of PMA/ionomycin, values were enhanced, but again only positive for the corresponding immunizing Ag (Supplemental Fig. 1B). Indeed, when cells were stimulated with PSBP alone, intracellular cytokine staining revealed few actively cytokine-producing cells. However, a brief incubation with PMA plus ionomycin unmasked substantial numbers of $CD4^+$ cells capable of producing IFN-γ or IL-17.

Ag specificity could also be shown by adoptive transfer experiments (Supplemental Fig. 1C). Indeed, when PAg- or OVA-immunized mice were euthanized and spleen cells were first in vitro stimulated with PSBP or OVA and then purified stimulated $CD3^+$ cells were adoptively transferred to NOD-SCID mice, the presence of $CD3^+$ cells in the prostate was only detected in NOD-SCID mice recipients of $CD3^+$ from PAg-immunized mice (Supplemental Fig. 1D, 1E). No $CD3^+$ cells were detected in the pancreas of NOD-SCID mice recipients of T cells from PAg-immunized mice. Furthermore, no $CD3^+$ cells were detected in the prostate or the pancreas of NOD-SCID mice recipients of $CD3^+$ cells from OVA-immunized mice (Supplemental Fig. 1E). These results showed that PAg immunized NOD mice, but no OVA-immunized NOD mice, exhibited peripheral T cells able to secrete IFN-γ and IL-17 in response to PSBP stimulation, and also able to home and infiltrate the prostate gland where their specific Ag is expressed.

Altogether, these results show that EAP induction in NOD mice is accompanied by a specific Th1/Th17 cell response and marked inflammatory lesions in prostatic tissue. In contrast, EAP in BALB/c mice is characterized by the induction of specific Th17 cells in lymphoid tissues that are unable to infiltrate the gland.

EAP induction in IFN-γ–deficient NOD mice

Strong differences in the genetic background between NOD and BALB/c mice and the marked up increase in IFN-γ–secreting cells in

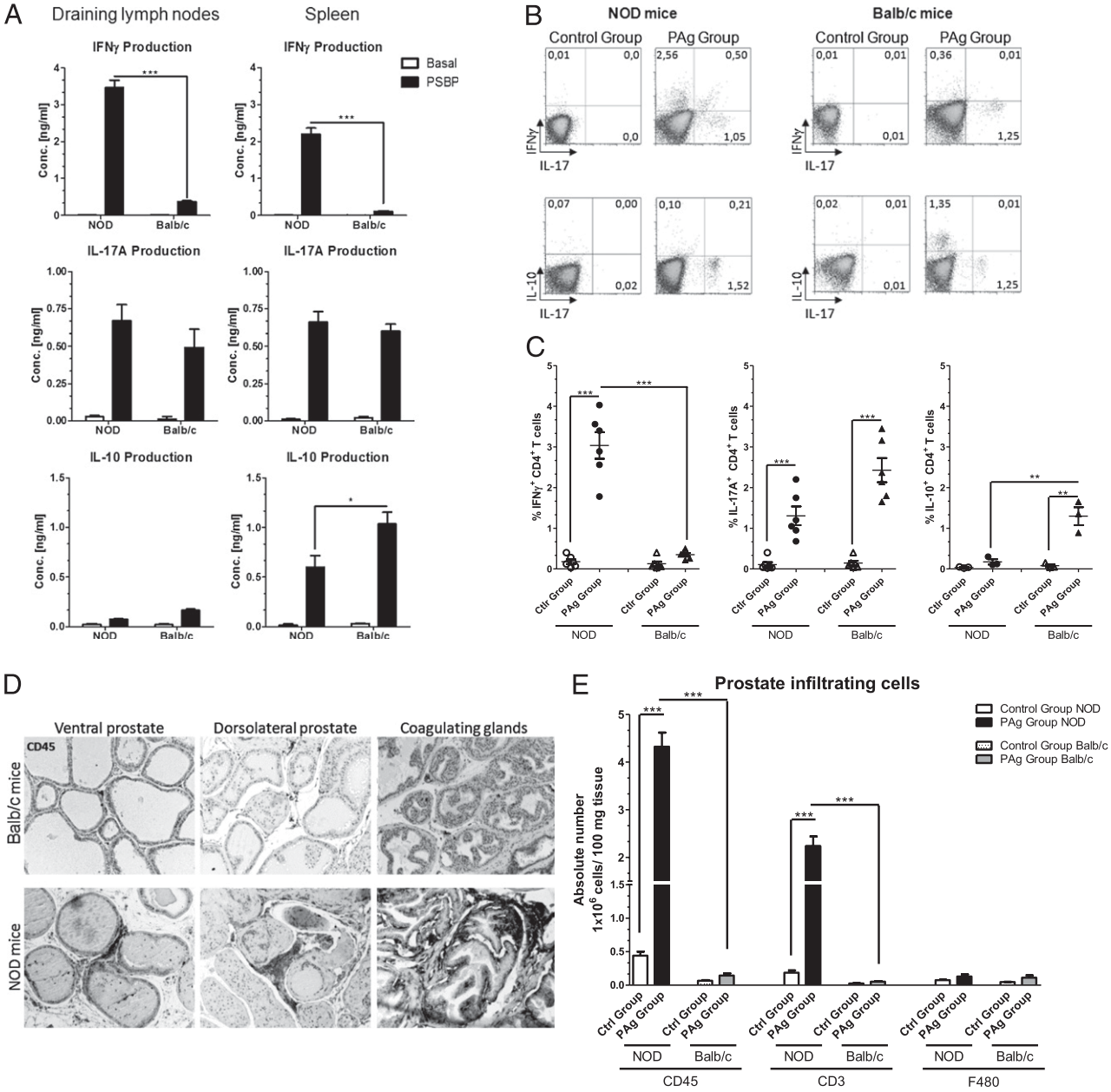

FIGURE 1. Prostate-specific Th1 and Th17 cells are induced in mice with differential susceptibility to EAP induction. NOD and BALB/c mice were immunized with PAg emulsified in CFA or CFA alone, euthanized at day 24 after immunization, and lymphoid organs and the prostate were obtained. Spleen or prostate draining LN mononuclear cells from NOD and BALB/c mice were cultured for 72 h in the presence of PSBP or medium. (**A**) Cytokine secretion in culture supernatants measured by ELISA. Data are shown as mean ± SEM, $n = 5$ per group, representative of three independent experiments. (**B**) Representative intracellular staining for IL-10, IL-17A, and IFN-γ was performed on spleen mononuclear cells stimulated with PSBP for 72 h. Shown data are cells gated in the $CD4^+$ cell population. (**C**) Percentages of IFN-γ^+CD3^+, IL-10^+CD3^+, and IL-17^+CD3^+ spleen cells from animals of control or PAg groups. (**D**) Representative immunohistochemistry assays for $CD45^+$ cells in prostate tissue sections from immunized NOD and BALB/c mice. Original magnification ×200. (**E**) Flow cytometry analysis of prostate-infiltrating cells from NOD and BALB/c mice. Mononuclear cells isolated from digested prostate glands were counted excluding dead cells and then stained for CD45, CD3, and F480. Data are shown as mean ± SEM, $n = 5$ per group, and are representative of three independent experiments. Statistical analysis was performed using one-way (A) and two-way ANOVA (C, E). $^*p < 0.05$, $^{**}p < 0.01$, $^{***}p < 0.001$.

mice susceptible to EAP induction led us to investigate Th-associated pattern and EAP susceptibility in mice deficient in IFN-γ. As expected, NOD–IFN-$\gamma^{-/-}$ mice did not develop specific IFN-γ–producing cells but exhibited comparable frequencies of specific IL-17– and IL-10–producing cells when compared with immunized wild type NOD mice (Fig. 2A, 2B). Similar to that observed in BALB/c mice, simple positive $CD4^+$IL-17^+ and $CD4^+$IL-10^+ T cells were detected in immunized NOD–IFN-$\gamma^{-/-}$ mice in lymphoid tissues (Fig. 2B). In contrast, immunized NOD–IFN-$\gamma^{-/-}$ mice showed comparable levels of TGF-β–, IL-5–, and IL-13–secreting cells after in vitro PSBP stimulation when compared with the ones observed in NOD mice (data not shown). Absent or negligible amounts of leukocyte infiltration were observed in the prostate of control and immunized NOD-IFN-$\gamma^{-/-}$ mice (Fig. 2C, 2D). These results indicate that NOD–IFN-$\gamma^{-/-}$ and BALB/c mice develop a similar pattern of prostate-specific immune response characterized by the induction of specific Th17 cells in spleen and draining LNs that are unable to infiltrate the prostate (Fig. 1C).

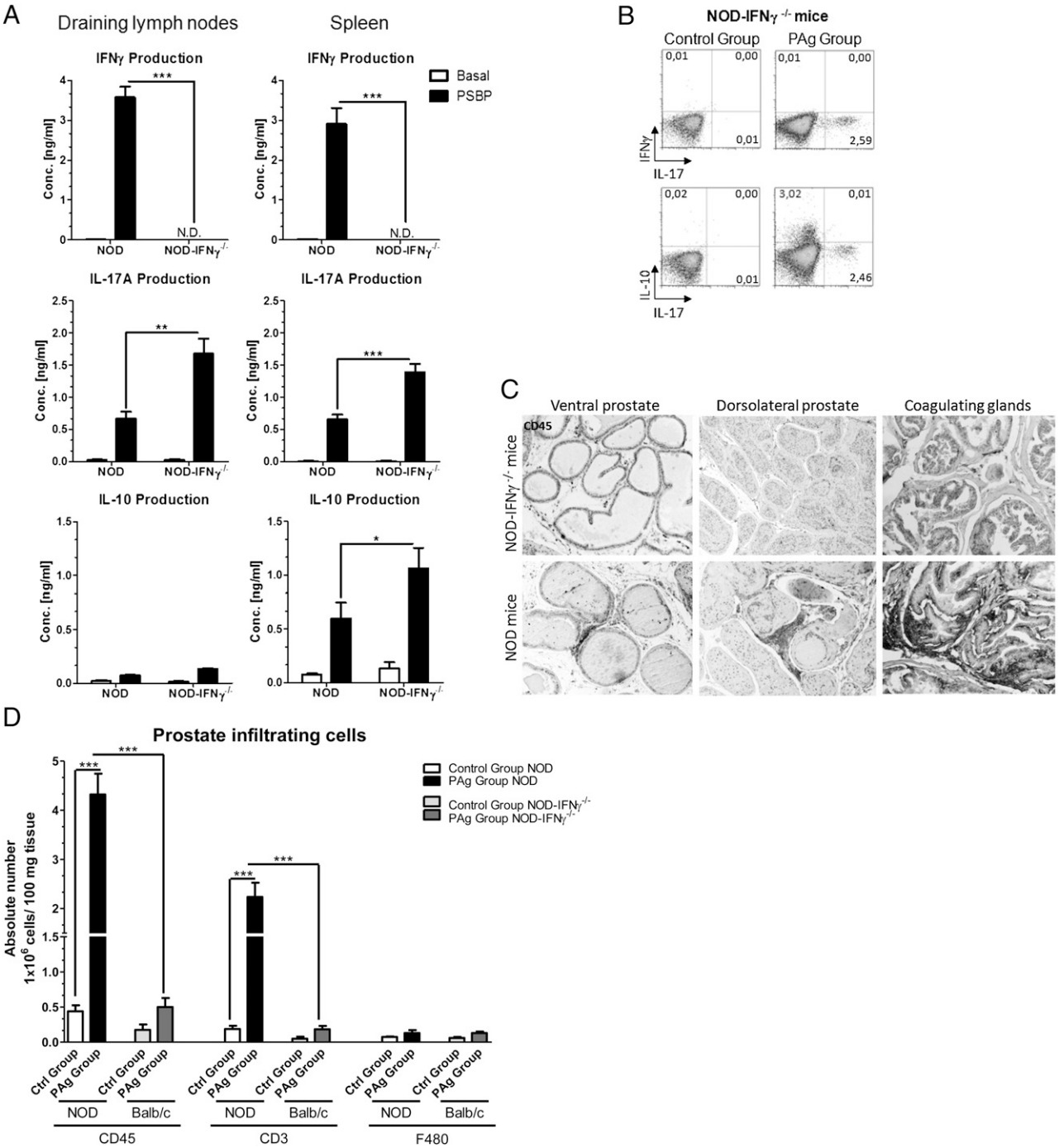

FIGURE 2. EAP induction in IFN-γ–deficient NOD mice. NOD–IFN-$\gamma^{-/-}$ mice were immunized with PAg emulsified in CFA or CFA alone, euthanized at day 24 after immunization, and lymphoid organs and the prostate were obtained. Spleen or prostatic draining LN mononuclear cells were cultured for 72 h in presence of PSBP or medium. (**A**) Cytokine secretion in culture supernatants measured by ELISA. Data are shown as mean ± SEM, $n = 5$ per group, representative of three independent experiments. (**B**) Intracellular staining for IL-10, IL-17A, and IFN-γ was performed on spleen mononuclear cells stimulated with PSBP for 72 h. Shown data are cells gated in the $CD4^+$ cell population. (**C**) Representative immunohistochemistry assays for $CD45^+$ cells in prostate tissue sections from immunized NOD and NOD–IFN-$\gamma^{-/-}$ mice. Original magnification ×200. (**D**) Flow cytometry analysis of prostate-infiltrating cells from NOD and NOD–IFN-$\gamma^{-/-}$ mice. Mononuclear cells isolated from digested prostate glands were counted excluding dead cells and then stained for CD45, CD3, and F480. Data are shown as mean ± SEM, $n = 5$ per group, and are representative of three independent experiments. Statistical analyses were performed using one-way (A) and two-way ANOVA (D). $^*p < 0.05$, $^{**}p < 0.01$, $^{***}p < 0.001$.

Chemokine receptor expression of specific T cells from NOD and NOD–IFN-$\gamma^{-/-}$ mice

T cell differentiation is accompanied by the expression of chemokine receptors responsible for T cell subset recruitment to and extravasation at inflammation sites (22). Although literature data are not yet conclusive, several authors have associated chemokine receptor expression to different Th subsets (23). It has been postulated that CXCR3 and CCR5 are preferentially expressed on Th1 cells, whereas CCR3, CCR4, and CCR8 are expressed on Th2 cells (27). More recently, CCR6 distinguishes the Th17 subset, although there is also evidence that Th17 cells may express CCR4, CCR2, and CCR9.

We next investigated the expression of CXCR3, CCR5, CCR4, and CCR6 in spleen T cells from NOD and NOD–IFN-$\gamma^{-/-}$ mice. To do that, we cultured spleen cells from control or immunized mice in the presence of PSBP or medium alone. T cells from control and immunized mice from both strains cultured in the presence of medium showed almost null levels of expression of chemokine receptors. However, a high frequency of $CXCR3^+$ $CCR5^+$ cells with also important quantities of $CCR6^+$ cells and low amounts of $CCR4^+$ cells were detected when analyzing $CD4^+$ T cells from immunized NOD mice cultured in the presence of the autoantigen PSBP (Fig. 3A, 3B). In contrast, $CD4^+$ T cells from immunized NOD–IFN-$\gamma^{-/-}$ mice cultured in the presence of PSBP were mainly $CCR6^+$ simple positive, showing no expression of CXCR3, CCR5, or CCR4 (Fig. 3A, 3B). The expression of the chemokine receptors on T cells from control NOD and NOD–IFN-$\gamma^{-/-}$ mice revealed percentages ranging between 0.01 and 0.76 for all chemokine receptors assayed after in vitro PSBP stimulation (Fig. 3).

These results showed that peripheral specific T cells from immunized NOD mice express Th1-associated chemokine receptors, whereas T cells from immunized NOD–IFN-$\gamma^{-/-}$ mice express chemokine receptors associated to Th17 cells.

Chemokine expression levels in prostate tissue from NOD and NOD–IFN-$\gamma^{-/-}$ mice

Chemokines have essential roles in the recruitment of leukocytes into inflamed tissues. There is very limited information about chemokines and chemokine receptors involved in the recruitment of

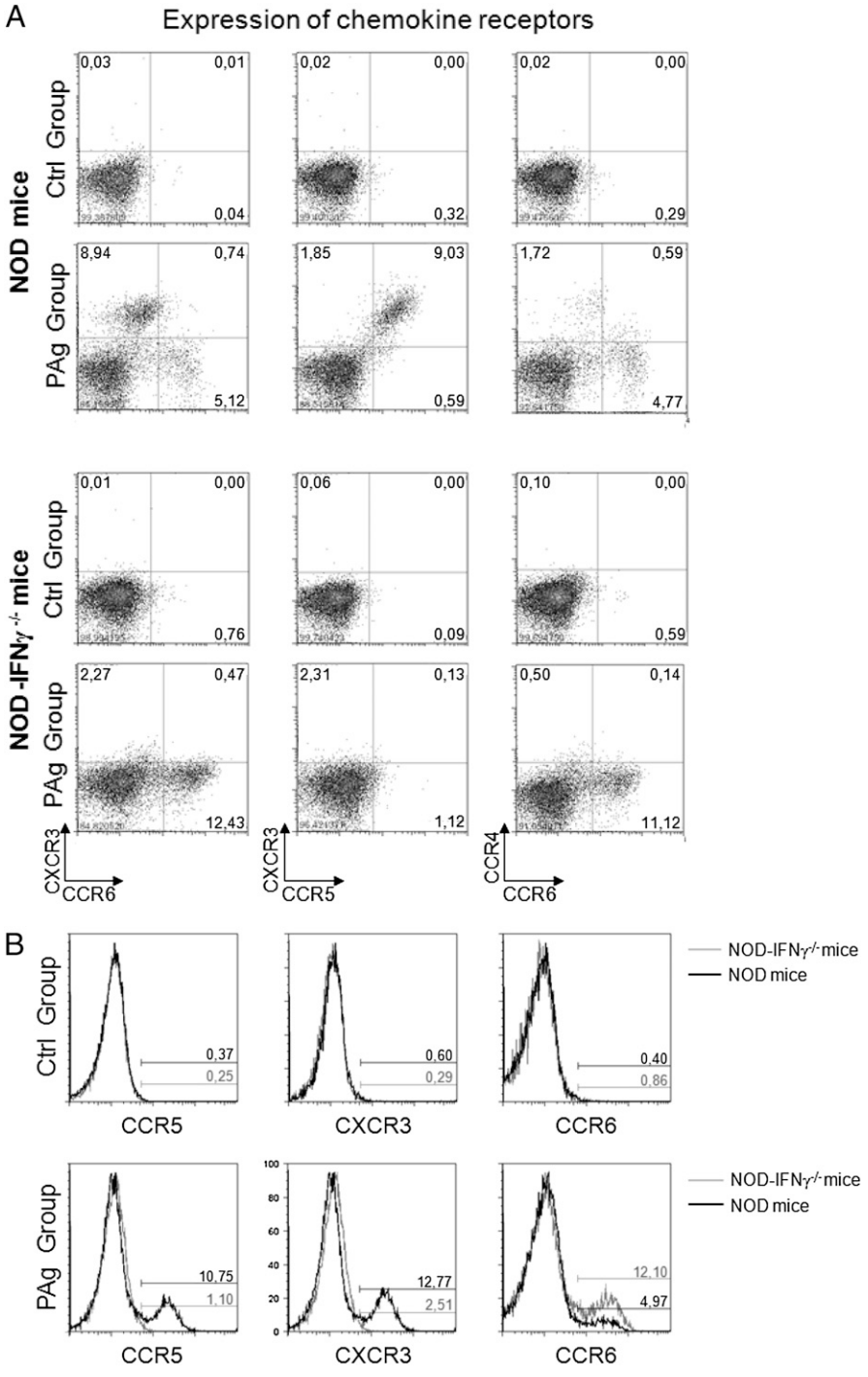

FIGURE 3. Prostate-specific T cells from immunized NOD and NOD–IFN-$\gamma^{-/-}$ mice express different patterns of chemokine receptors. (**A** and **B**) NOD and NOD–IFN-$\gamma^{-/-}$ mice were immunized with PAg emulsified in CFA (PAg groups) or CFA alone (control groups) and sacrificed at day 24 after immunization. Spleen mononuclear cells were cultured for 72 h in the presence of PSBP; then surface staining for chemokines receptors was performed. Numbers indicate percentage among gated $CD4^+$ T cells. Data are representative of three independent experiments. Numbers indicate the percentage of cells in each quadrant.

immune cells to the prostate gland. Considering that, we analyzed the expression of different chemokine ligands for CXCR3, CCR5, and CCR6 in prostate tissue from control and immunized wild type NOD or NOD–IFN-$\gamma^{-/-}$ mice using a protein array. Regarding known ligands for CXCR3, control NOD mice showed detectable levels of CXCL11 and CXCL9, whereas none of these chemokines was detectable in control NOD–IFN-$\gamma^{-/-}$ mice (Fig. 4A). CXCL9, CXCL10, and CXCL11 showed increased expression levels in prostate tissue from immunized NOD mice, but not in immunized NOD–IFN-$\gamma^{-/-}$ mice, with CXCL10 being the chemokine mostly increasingly expressed (15-fold increase; Fig. 4A, Supplemental Fig. 2).

Regarding ligands for CCR5, control NOD mice exhibited high levels of CCL4 and detectable levels of CCL3 and CCL5 expression, whereas only CCL4 could be detected in control NOD–IFN-$\gamma^{-/-}$ prostate samples. The expression of CCL3 and CCL5 was significantly increased in prostate tissue from immunized NOD mice, whereas CCL4 showed high levels in both immunized and control NOD mice (Fig. 4B). The expression of CCL3 and CCL5 was almost null in control or immunized NOD–IFN-$\gamma^{-/-}$ mice, whereas CCL4 was either increased in control or immunized NOD–IFN-$\gamma^{-/-}$ mice, although at lower levels when compared with control or immunized wild type NOD mice (Fig. 4B). When chemokine expression levels detected in control and immunized mice from both strains were compared, it was shown that CCL3 and CCL5 were 2.5- and 6-fold, respectively, increased in prostate tissue from immunized NOD mice (Supplemental Fig. 2).

Regarding CCL20, a chemokine ligand for CCR6, greater levels were detected in prostate samples from immunized NOD mice, whereas immunized NOD–IFN-$\gamma^{-/-}$ mice also showed increased amounts when compared with control mice (Fig. 4C), showing a 3.7- and 2-fold increase, respectively (Supplemental Fig. 2).

Using the same protein array, we also searched for the expression of some cytokines (IL-10, IL-17A, IFN-γ, and IL-12p70) in prostate tissue samples under study. As shown in Fig. 4D, control mice from both strains showed detectable levels of IL-12p70, whereas immunized NOD mice exhibited greater levels of IL-12p70, IFN-γ, and IL-17 when compared with immunized NOD–IFN-$\gamma^{-/-}$ mice, showing a state of inflammation in the prostate from NOD mice. Although IL-12p70 and IFN-γ expression increased 7 and 20 times, respectively, in immunized NOD mice when compared with control NOD mice, none of the inflammatory cytokines analyzed showed more than a 2-fold increase in immunized NOD–IFN-$\gamma^{-/-}$ mice (Fig. 4D, Supplemental Fig. 2). Altogether, these results showed that after immunization, NOD mice showed strongly increased expression levels of CCR5 and CXCR3 ligands accompanied by increased levels of inflammatory cytokines in prostatic tissue. These data indicate that in a steady-state, prostates from NOD mice express some chemokines and cytokines that may favor a baseline inflammatory status.

Prostate-specific T cells from NOD and NOD–IFN-$\gamma^{-/-}$ mice show differential capabilities of homing to and infiltrating the prostate gland

To study whether specific T cells from immunized NOD and NOD–IFN-$\gamma^{-/-}$ mice were able to migrate to and infiltrate the prostate tissue, we sorted $CD3^+$ cells after in vitro autoantigen stimulation and then transferred 1×10^6 $CD3^+$ T cells to NOD-SCID recipients (Fig. 5A). Fifteen or 30 d after adoptive transfer, we searched for the presence of $CD3^+$ cells in different organs of NOD-SCID recipient mice. As shown in Fig. 5B and Supplemental Fig. 3, $CD3^+$ cells from immunized NOD mice could be detected in spleen, prostate nondraining LNs, prostate draining LNs, and the prostate, but not in the pancreas of NOD-SCID recipients (Fig. 5B), showing that $CD3^+$ T cells circulated and infiltrated the

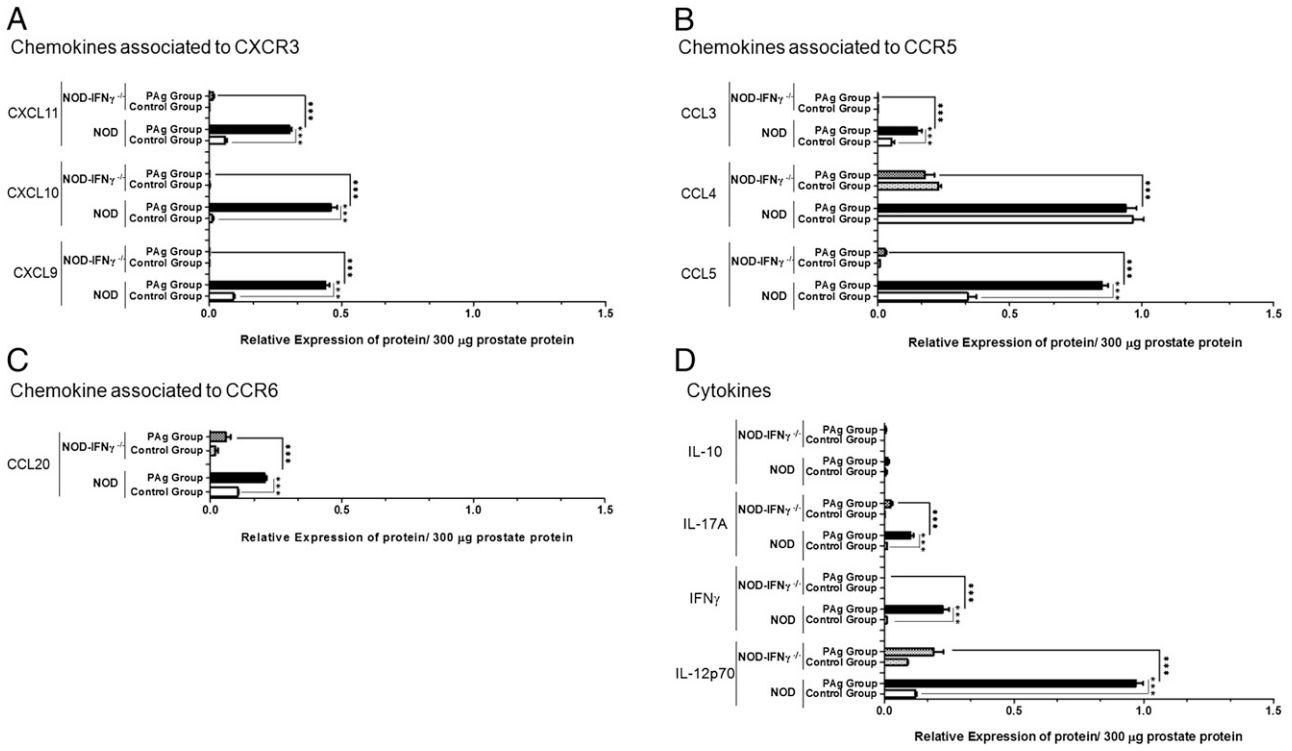

FIGURE 4. Relative protein expression of chemokines in prostate tissue from control and immunized NOD and NOD–IFN-$\gamma^{-/-}$ mice. (**A**–**D**) Prostates from PAg or CFA alone immunized animals were obtained and excised at day 24 after immunization, and protein levels of chemokines in tissue samples were measured. (A) Chemokines associated to CXCR3. (B) Chemokines associated to CCR5. (C) Chemokine associated to CCR6. (D) Cytokines expressed in prostate tissue. Statistical analysis was performed using two-way ANOVA. ***$p < 0.001$.

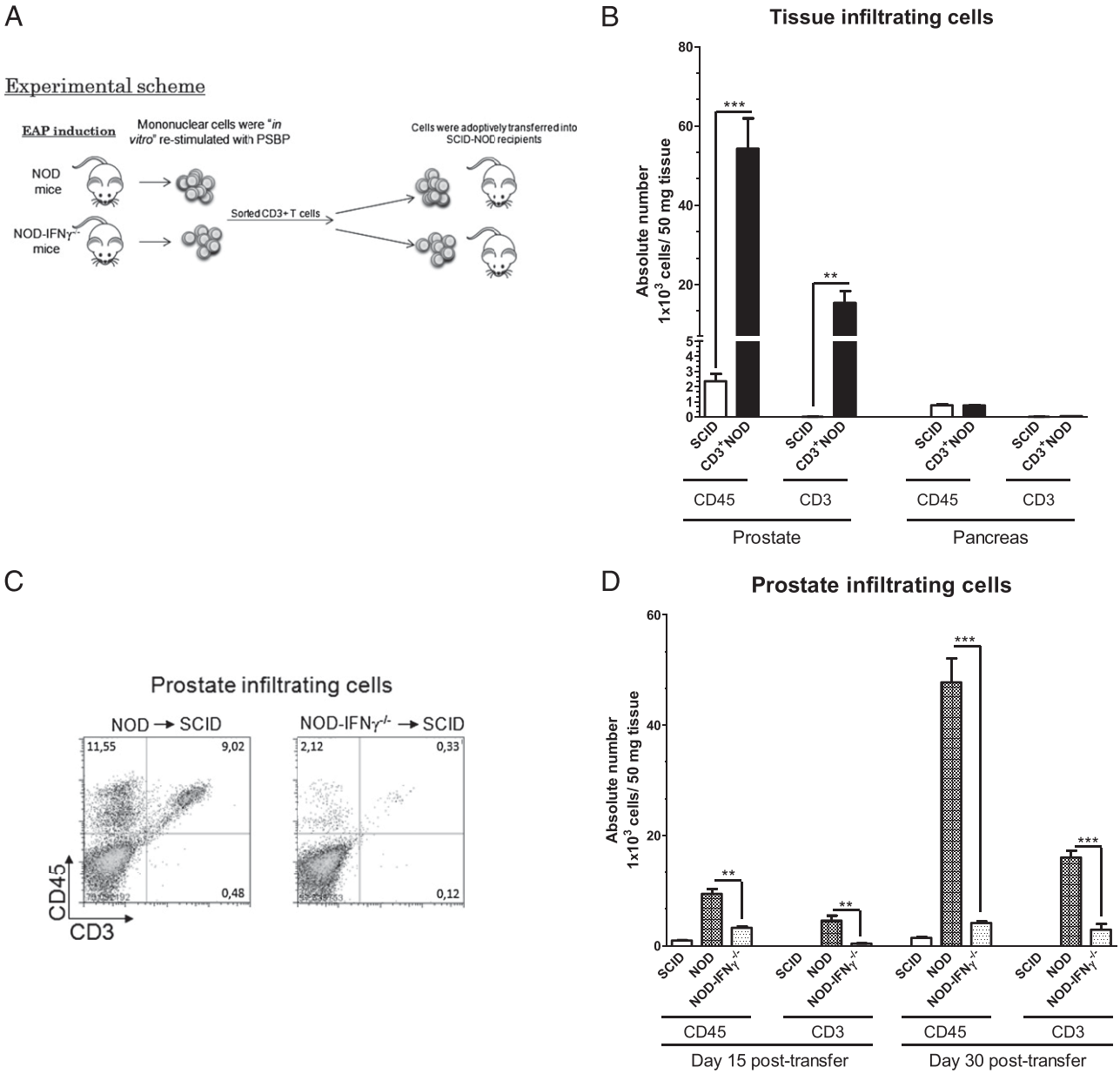

FIGURE 5. PSBP-specific T cells from NOD and NOD–IFN-$\gamma^{-/-}$ mice show different capabilities of homing to the prostate gland. Mononuclear cells from PAg immunized NOD and NOD–IFN-$\gamma^{-/-}$ mice were in vitro restimulated with the autoantigen PSBP for 72 h; then 1×10^6 sorted $CD3^+$ T cells were i.v. transferred into NOD-SCID recipients. The prostate and the pancreas were collected on days 15 and 30 after transfer. Live cells were counted and flow cytometry was preformed to evaluate leukocyte infiltration in the glands. (**A**) Experimental scheme. (**B**) Presence of leukocytes in the prostate and pancreas from NOD-SCID recipients on day 30 after transfer. (**C**) Representative flow cytometry plots of the analysis of leukocyte infiltration in NOD-SCID recipient mice on day 30 after transfer. (**D**) Absolute number of $CD45^+$ and $CD3^+$ cells in the prostate gland from NOD-SCID recipients at days 15 and 30 after transfer. White bars represent $CD45^+$ and $CD3^+$ values in the prostate from nontransferred NOD-SCID mice. Data are shown as mean ± SEM, $n = 2$ recipients mice per group, and are representative of three independent experiments. Statistical analysis was performed using one-way ANOVA. $^{**}p < 0.01$, $^{***}p < 0.001$.

prostate gland. We detected $CD3^+$ T cells in spleen, prostate draining LNs, and nondraining LNs at both time points assayed (Supplemental Fig. 3). Lower amounts of $CD3^+$ T cells were detected in spleen from recipients adoptively transferred with $CD3^+$ T cells from immunized NOD mice. No significant differences were detected in the number of $CD3^+$ T cells in nondraining LNs from NOD-SCID recipients of $CD3^+$ T cells from immunized NOD or NOD–IFN-$\gamma^{-/-}$ mice either at day 15 or 30 after transfer (Supplemental Fig. 3). Interestingly, higher numbers of $CD3^+$ T cells were detected in draining LNs from NOD $CD3^+$ cell recipients than in draining LNs from NOD–IFN-$\gamma^{-/-}$ $CD3^+$ cell recipients (Supplemental Fig. 3).

We also analyzed the presence of $CD3^+$ T cells in the prostate gland. With that purpose, cytometry analysis was performed in prostates from NOD-SCID recipient mice. Increased quantities of $CD45^+$ and $CD3^+$ cells were observed at day 15 after transfer, with increasing amounts at day 30 only in the prostates from NOD-SCID mice that received $CD3^+$ T cells from immunized wild type NOD mice (Fig. 5C, 5D). At day 30, an increase of both $CD3^+$ and $CD45^+$ cells was observed, suggesting the recruitment of other immune cells from the host mice (Fig. 5C, 5D). Interestingly, prostate tissue samples from NOD-SCID recipients of $CD3^+$ T cells from immunized NOD–IFN-$\gamma^{-/-}$ mice showed minimal amounts of $CD3^+$ or $CD45^+$ cells.

Altogether, these results indicate that after immunization, NOD mice develop prostate-specific T cells that secrete IFN-γ, IL-17, and express mainly CXCR3 and CCR5. These cells are able to migrate to and infiltrate the prostate gland, and after that are also able to induce the recruitment of other immune cells. In contrast, immunized NOD–IFN-$\gamma^{-/-}$ mice also develop prostate-specific T cells with a different pattern of cytokine secretion. These cells mainly express CCR6 and circulate, but do not infiltrate, the prostate gland at the time points assayed.

Chemokine receptor expression and ability to home to the prostate gland of T cells from NOD–IFN-$\gamma^{-/-}$ mice after treatment/stimulation with rIFN-γ

Considering the importance of IFN-γ in EAP, we performed experiments stimulating T cells from immunized NOD–IFN-$\gamma^{-/-}$ mice with the autoantigen PSBP plus rIFN-γ in vitro; then these cells were analyzed for the expression of chemokine receptors and their ability to home to the prostate. Interestingly, a high frequency of $CXCR3^+CCR5^+$ cells was observed in $CD3^+$ T cells from immunized NOD–IFN-$\gamma^{-/-}$ mice after autoantigen plus rIFN-γ stimulation (Fig. 6A). An important diminution in the number of $CCR6^+$ cells was also observed (Fig. 6A). Interestingly, when these cells were sorted and transferred to NOD-SCID mice, similar migration ability to the one observed in cells from immunized wild type NOD mice was detected (data not shown). After in vitro stimulation with the autoantigen plus rIFN-γ, these cells became capable of infiltrating the prostate and also of inducing the recruitment of more $CD45^+$ cells from the recipient (Fig. 6B, 6C). In other experiments, we treated immunized NOD–IFN-$\gamma^{-/-}$ mice with rIFN-γ as described in *Materials and Methods* and Fig. 6D. Mirroring that previously observed in in vitro experiments, in vivo rIFN-γ treatment of immunized NOD–IFN-$\gamma^{-/-}$ mice induced the expression of CXCR3 and CCR5 in $CD3^+$ T cells from secondary lymphoid organs (data not shown). More interestingly, the treatment induced a strong increase in the leukocyte infiltration of the prostate gland from these mice (Fig. 6E, 6F).

These results showed that specific $CD3^+$ T cells from NOD–IFN-$\gamma^{-/-}$ mice, although unable to produce IFN-γ, after treatment with rIFN-γ they do express CXCR3 and CCR5, and migrate to and infiltrate the prostate gland. It is important to highlight that these cells do not secrete IFN-γ, but they were still capable of homing to the prostate gland and of inducing inflammation and recruitment of other immune cells. Altogether, our results suggest that the expression of CXCR3 more than the secretion of IFN-γ is the critical task that specific T cells need to achieve to infiltrate the prostate gland and establish an inflammatory milieu.

The expression of chemokine receptor CXCR3 is crucial for conferring prostate-specific T cells the capability of infiltrating the prostate gland

Finally, we performed adoptive transfer experiments with total $CD3^+$, $CXCR3^+CD3^+$, or $CXCR3^-CD3^+$ cells from immunized NOD mice sorted after in vitro autoantigen stimulation. Cells were transferred to NOD-SCID recipients, and 30 d later the presence of $CD3^+$ cells in prostate tissue was analyzed. As shown in Fig. 7A, significant amounts of $CD3^+$ cells were detected in the prostates from $CXCR3^+CD3^+$ cells recipients, whereas NOD-SCID mice that received $CXCR3^-CD3^+$ cells showed scarce quantities of $CD3^+$ cells in the prostate. In addition, not only $CD3^+$ cells could be detected in the prostate from $CXCR3^+CD3^+$ cells recipients, but also important amounts of $CD45^+$ cells suggesting the recruitment of host leukocytes to the target organ.

To determine whether blockade of CXCR3 chemokine receptor modulates prostate infiltration, we investigated the effect of a treatment with a nonpeptide chemokine receptor antagonist for CXCR3 and CCR5 (named TAK-779) on the ability of transferred T cells to infiltrate the prostate gland and to induce inflammation. As shown in Fig. 7B, NOD-SCID mice transferred with specific $CD3^+$ T cells from immunized NOD mice and then treated with TAK-779 exhibited lesser quantities of $CD3^+$ cells infiltrating the prostate when compared with vehicle-treated recipients. The blockade of CXCR3 chemokine receptor had also effects on other inflammatory cell recruitment, because $CD45^+$ cells and $CD11b^+$ cells were also diminished in prostate tissue from TAK-779–treated recipient mice. Moreover, TAK-779 treatment had no effects on leukocyte infiltration present in the pancreas of NOD-SCID recipients (Fig. 7C).

These results showed that specific T cells induced in periphery must express CXCR3 to home to the prostate gland. Once in the prostate and after further autoantigen stimulation, specific cells may release chemokines and cytokines that would subsequently induce the recruitment of other immune cells.

Discussion

The pathogenesis of many autoimmune diseases has long been thought to be orchestrated by Th1 cells. The discovery that IL-23, and not IL-12, was indispensable for EAE and its association with the differentiation and expansion of Th17 cells marked the beginning of a new era in the understanding of autoimmune pathogenesis (20). Since then, Th17 cells have been implicated in the pathogenesis of several autoimmune diseases, including multiple sclerosis and rheumatoid arthritis. In the case of autoimmune diabetes, the function of Th17 cells has been a topic of much debate (28–30). Some researchers have argued for a critical role of Th17 cells especially in later effector processes (28), although others have cautioned about possible misinterpretations of findings from Th17 transfer experiments because of the conversion to or expansion of Th1 cells (29, 31). Therefore, Th17 cells have been identified as major players in some autoimmune processes and with contradictory functions in others.

In this report, we provided evidence demonstrating that after EAP induction, the susceptible NOD mice strain develops both Th1- and Th17-specific cells. These T cells are able to produce IFN-γ and IL-17 in response to PSBP, but not in response to OVA. Moreover, PAg-immunized animals, but not OVA-immunized animals, showed marked leukocytic infiltration in the prostate, mainly composed of T cells and macrophages. Interestingly, mice from the resistant BALB/c strain, as well as NOD-IFN-$\gamma^{-/-}$ mice, exhibited only specific Th17 cells in periphery but no infiltration or histological alterations in the target organ after immunization. These IL-17–producing cells were not double producers of IL-10, indicating that these cells were not the regulatory Th17 cells previously reported in EAE (26, 31). IL-10–producing $CD4^+$ T cells were detected in wild type NOD and also in NOD–IFN-$\gamma^{-/-}$ mice. In addition, similar levels of TGF-β, IL-5, and IL-13 were detected when compared with the ones observed in immunized wild type NOD mice. These results do not allow discarding possible differences in immune regulation between both strains. However, adoptive transfer experiments demonstrated that T cells from NOD–IFN-$\gamma^{-/-}$ mice were actually unable to transfer the disease. The fact that NOD–IFN-$\gamma^{-/-}$ mice do not develop autoimmune prostatitis and the failure of T cells obtained from these mice to transfer the disease to NOD-SCID mice argue again for a fundamental role of IFN-γ and Th1 cells in EAP.

It has been postulated that the characteristic Th17 response is not necessarily central to all T cell–driven autoimmune disorders. Some reports have shown that IL-17–producing cells were found to inhibit diabetes development in NOD mice, as well as in Bio-

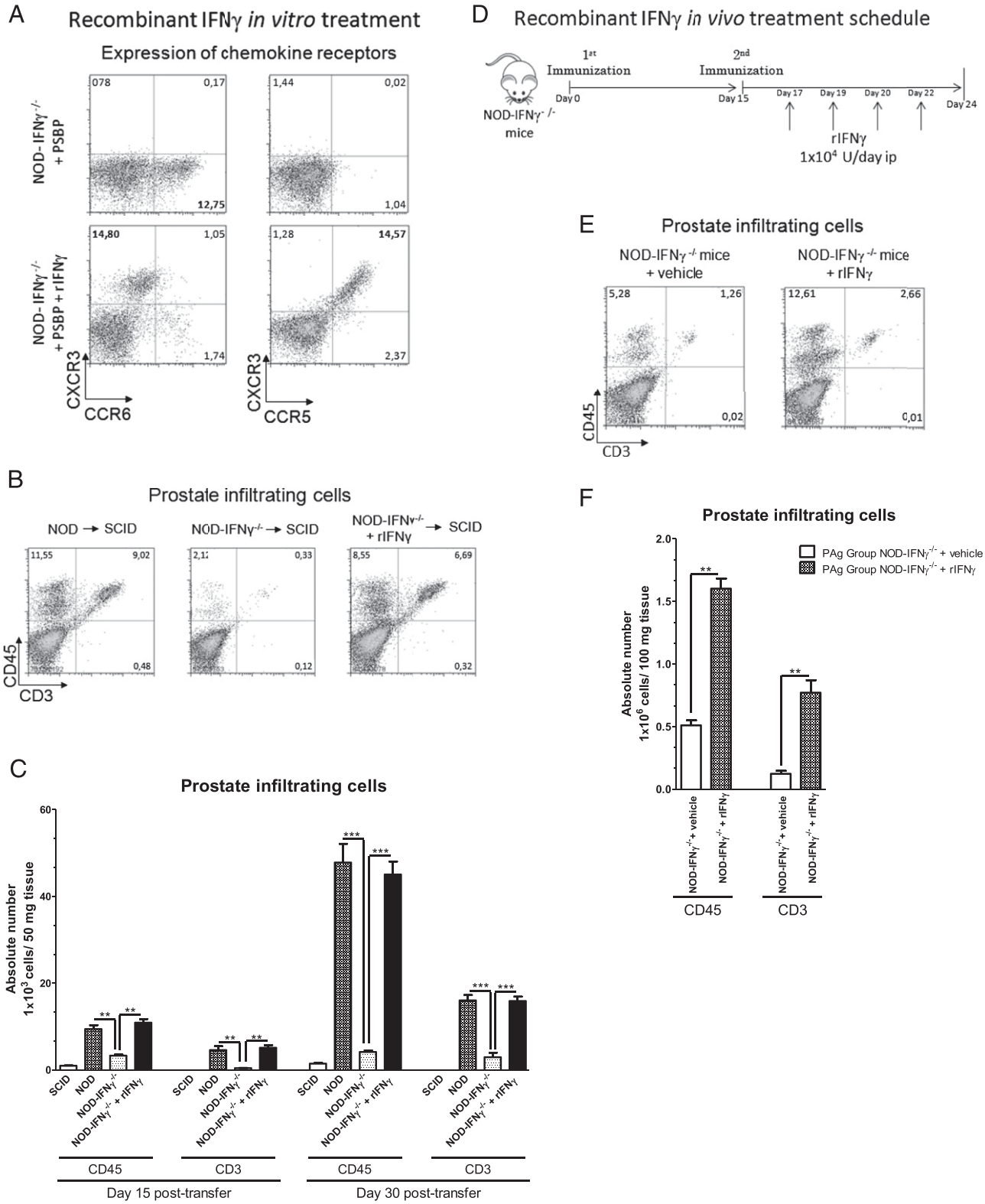

FIGURE 6. IFN-γ affects the homing of PSBP-specific T cells to the prostate. Spleen mononuclear cells from PAg immunized NOD–IFN-$\gamma^{-/-}$ mice were cultured in the presence of PSBP alone or plus rIFN-γ for 72 h. Then cells were stained for surface expression of different chemokine receptors. (**A**) Flow cytometry analysis of CCR6, CCR5, and CXCR3 in gated $CD4^+$ T cells. Data are representative of three independent experiments. (**B**) Flow cytometry analysis of prostate tissue from recipients transferred with T cells from PAg immunized NOD and NOD–IFN-$\gamma^{-/-}$ mice. Mononuclear cells isolated from the prostate gland were counted excluding dead cells and then stained for CD45 and CD3. (**C**) Absolute number of $CD45^+$ and $CD3^+$ cells in the prostate gland from NOD-SCID recipients at days 15 and 30 after transfer. Data are shown as mean ± SEM, $n = 4$ per group, and are representative of three independent experiments. (**D**) Experimental scheme. (**E**) Flow cytometry analysis of prostate tissue from immunized NOD–IFN-$\gamma^{-/-}$ mice i.p. treated with rIFN-γ. Mononuclear cells isolated from prostate tissue were counted excluding dead cells and then stained for $CD45^+$ and $CD3^+$ cells. (**F**) Absolute number of CD45 and CD3 in prostate tissue from immunized NOD–IFN-$\gamma^{-/-}$ mice i.p. treated with rIFN-γ. Data are shown as mean ± SEM, $n = 4$ per group, and are representative of three independent experiments. Statistical analysis was performed using one-way ANOVA. $^{**}p < 0.01$, $^{***}p < 0.001$.

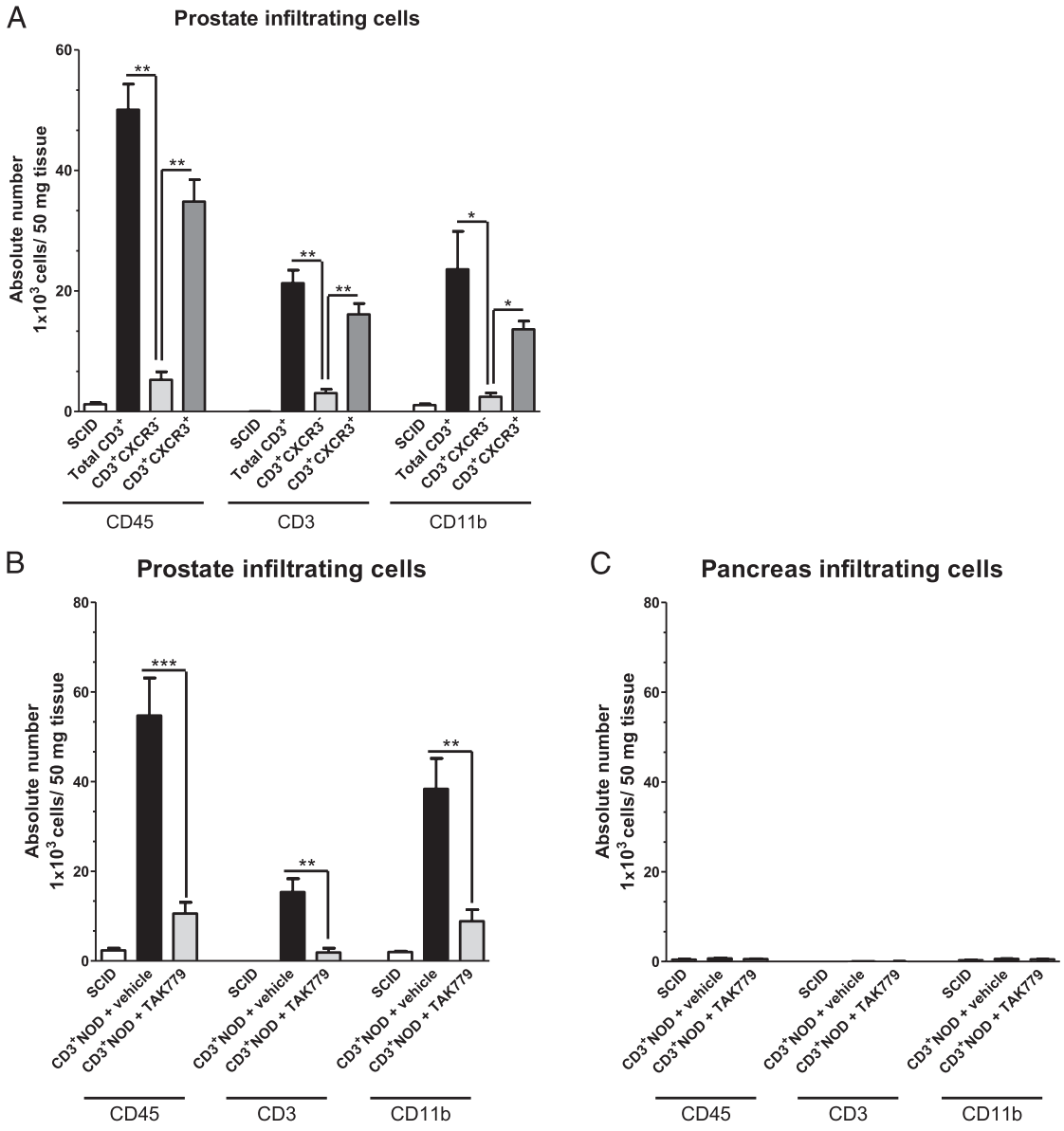

FIGURE 7. Expression of CXCR3 in prostate-specific T cells is essential for their homing to the prostate. (**A**) Spleen mononuclear cells from PAg immunized NOD mice were sorted into $CD3^+$, $CD3^+CXCR3^+$, and $CD3^+CXCR3^-$ fractions after PSBP in vitro stimulation. Sorted fractions were i.v. transferred into NOD-SCID recipients. Prostate glands were collected on day 30 after transfer and processed as previously described. Absolute number of $CD45^+$, $CD3^+$, and $CD11b^+$ cells in the prostate gland from NOD-SCID recipients at day 30 after transfer are depicted; white bars represent $CD45^+$, $CD3^+$, and $CD11b^+$ cell values in prostate tissue of a nontransferred NOD-SCID mice. Data are shown as mean ± SEM, $n = 2$ recipient mice per group, and are representative of three independent experiments. (**B** and **C**) Sorted $CD3^+$ T cells from immunized NOD mice were transferred to NOD-SCID mice as described. After transfer, recipient mice were treated with TAK-779 or vehicle. Absolute number of $CD45^+$, $CD3^+$, and $CD11b^+$ cells in the prostate gland (B) or the pancreas (C) from NOD-SCID recipients treated with TAK-779 or vehicle (day 30 after transfer). White bars represent $CD45^+$, $CD3^+$, and $CD11b^+$ cells values in prostate tissue from nontransferred NOD-SCID mice. Data are shown as mean ± SEM, $n = 3$ recipient mice per group, and are representative of two independent experiments. Statistical analysis was performed using one-way ANOVA. $^*p < 0.05$, $^{**}p < 0.01$, $^{***}p < 0.001$.

Breeding rats, in several contexts or have reported to have no effects at all (32–35). Indeed, Joseph et al. (36) have recently demonstrated that although IL-17 silencing in the NOD background reduces EAE severity, it does not alter diabetes susceptibility, showing that Th17 effector function may be dispensable in the pathogenesis of autoimmune diabetes. It has also been demonstrated that cosegregation of diabetes protection with a single gut resident commensal bacteria was associated with the emergence of a robust Th17 population in the gut (37). Kriegel et al. suggested that this population may impact diabetogenesis by inhibiting the islet-directed Th1 response (37), a notion compatible with a recent report that showed that Th17 cells inhibit Th1 effector cells in a colitis model (38). Our results suggest that Th17 effector function may be dispensable in the pathogenesis of autoimmune prostatitis.

The chemokine system provides cues for the recruitment of effector and regulatory cell subsets, and is central to the pathogenesis of inflammatory diseases (21). Chemokines direct leukocyte trafficking and positioning within tissues (23). In some autoimmune disorders, CXCL10 levels in the affected tissues correlated with local infiltration of T lymphocytes, suggesting that CXCR3/CXCL10 signaling plays an important role in the recruitment of T cells into the site of inflammation and autoimmune attack (39). Indeed, CXCR3/CXCL10 signaling has been impli-

cated in psoriasis, inflammatory bowel disease, rheumatoid arthritis, and autoimmune uveitis, but it has never been implicated in prostatitis to date. In addition, CCR6/CCL20 has been involved in the recruitment of T cells to the CNS or into the gut in chronic inflammatory conditions (40, 41). Because there is very scarce information about chemokines and chemokine receptors involved in the homing and recruitment of immune cells to the prostate gland, we investigated chemokines expressed in the prostate tissue and the pattern of chemokine receptors expressed by effector T cells. Our results showed that the prostate from control NOD mice expresses detectable levels of CXCL9, CXCL11, CCL5, CCL4, CCL20, IL-12p70, and IFN-γ, arguing for an inflammatory steady-state that may be involved in directing initial leukocyte trafficking and positioning within the prostate gland. It is known that once T cells become activated by the Ag, they change their pattern of homing receptors and can migrate to peripheral tissues. After different events, lymphocytes gain access to the tissue where their specific Ag is expressed. In this work, transfer of effector T cells to NOD-SCID mice showed that T cells from immunized NOD mice expressing CXCR3 and CCR5 were able to home to the prostate, but not to the pancreas, possibly directed by chemokines expressed in the NOD prostate and because of the expression of the specific Ags. On the contrary, T cells from immunized NOD–IFN-$\gamma^{-/-}$ mice expressing CCR6 were able to circulate within secondary lymphoid organs, but not to infiltrate the prostate of recipients. Interestingly, when effector T cells from NOD–IFN-$\gamma^{-/-}$ mice were in vitro cultured in the presence of rIFN-γ, they expressed CXCR3 and CCR5, and became capable of infiltrating the prostate and also of inducing the recruitment of host leukocytes. Moreover, in vivo treatment of NOD–IFN-$\gamma^{-/-}$ mice with rIFN-γ also induced the expression of CXCR3 on specific T cells and conferred the capability of infiltrating the prostate gland, suggesting that the expression of CXCR3 more than the ability to produce IFN-γ is the important feature that specific T cells need to achieve to be capable of infiltrating and establishing an inflammatory milieu in the target organ. CXCR3-expressing T cells migrated to and infiltrated the prostate in a much larger number than T cells not expressing this chemokine receptor. Moreover, the blockade of CXCR3 with a nonpeptide antagonist significantly inhibited prostate infiltration. However, because TAK-779 has also been described to block CCR5 and because $CXCR3^+$ T cells were also $CCR5^+$, we cannot exclude CCR5 contribution. In EAE, it has been reported that mice lacking CCR6 did develop Th17 responses but were highly resistant to the induction of the disease (42). EAE susceptibility was reconstituted by the transfer of wild-type T cells that entered into the CNS before disease onset and triggered massive CCR6-independent recruitment of effector T cells across activated parenchymal vessels (42).

It has been reported that a variety of chemokines are actively secreted within the prostatic microenvironment consequent to disruptions in normal tissue homeostasis because of the aging process and/or inflammatory responses (43). Chemokine secretion has been evaluated in both semen and expressed prostatic secretion from men with prostatitis showing that CXCL5 and CXCL8 were elevated in expressed prostatic secretion from men with bacterial prostatitis, CPPS, and asymptomatic inflammatory prostatitis (10, 44), chemokines that are both highly angiogenic and leukoattractant. In addition, CCL2 and CCL3 have also been postulated as biomarkers correlating with pelvic pain symptoms (45, 46). However, the expression of CXCR3 or CCR6 ligands in prostate tissue from patients bearing CCPS has not been investigated to date.

The EAP model developed in our laboratory has been successfully used to study CP/CPPS (4, 13). We consider our model to be valid and useful for improving the current understanding of the immune mechanisms involved in the pathogenesis of CP/CPPS and its consequences (14–16, 18, 19). In fact, many aspects of human disease have been reproduced in our model, although many others remain to be properly elucidated such as the identification of more autoantigens involved, immunodominant peptides, and the fine specificity of T cells infiltrating the prostate. Although we can presume that, if not all, most cells found infiltrating the prostate gland from recipients after adoptive transfer experiments are indeed PAg specific, for example, PSBP specific or specific to other not yet identified PAgs, we still cannot undoubtedly affirm that. However, the fact that recipient animals transferred with T cells from PAg-immunized animals, and not recipients transferred with T cells from OVA-immunized animals, developed the disease suggests that most T cells that home to and infiltrate prostate tissue are PAg specific. More conclusive evidence could be obtained in the near future when immunodominant peptide transgenic TCR mice, conjugated multimers, and systems for T cell in vivo tracking become available in the EAP model.

In this article, we have contributed to the current knowledge of chemokine and chemokine receptors involved in T cell homing to the prostate during an inflammatory process. We demonstrate for the first time, to our knowledge, the importance of CXCR3 in the development of autoimmune prostatitis and propose a new potential therapeutic target for CPPS treatment. These data may be useful in improving the understanding of how prostate infiltration occurs during inflammation and also may help in the design of possible therapeutic strategies to mitigate the damage in inflammatory conditions. The improvement in the current understanding of chemokine and chemokine receptors involved in the homing to the prostate may also have implications for other prevalent diseases that affect the prostate such as benign prostate hyperplasia and cancer.

Acknowledgments

We thank Dr. Diane Mathis and Christophe Benoist for providing the NOD–IFN-$\gamma^{-/-}$ [NOD.129S7 (B6)-IFN-γ^{tm1Ts}] and NOD-SCID (NOD.CB17-Prkdc^{scid}/J) mice. We thank Dr. Eliane Piaggio for helpful discussions and critical review of the manuscript. We also thank Paula Icely, Paula Abadie, and Pilar Crespo for excellent technical assistance.

Disclosures

The authors have no financial conflicts of interest.

References

1. Collins, M. M., R. S. Stafford, M. P. O'Leary, and M. J. Barry. 1998. How common is prostatitis? A national survey of physician visits. *J. Urol.* 159: 1224–1228.
2. Schaeffer, A. J. 2006. Clinical practice. Chronic prostatitis and the chronic pelvic pain syndrome. *N. Engl. J. Med.* 355: 1690–1698.
3. Krieger, J. N., L. Nyberg, Jr., and J. C. Nickel. 1999. NIH consensus definition and classification of prostatitis. *JAMA* 282: 236–237.
4. Rivero, V. E., R. D. Motrich, M. Maccioni, and C. M. Riera. 2007. Autoimmune etiology in chronic prostatitis syndrome: an advance in the understanding of this pathology. *Crit. Rev. Immunol.* 27: 33–46.
5. Motrich, R. D., M. Maccioni, R. Molina, A. Tissera, J. Olmedo, C. M. Riera, and V. E. Rivero. 2005. Presence of INFgamma-secreting lymphocytes specific to prostate antigens in a group of chronic prostatitis patients. *Clin. Immunol.* 116: 149–157.
6. Alexander, R. B., F. Brady, and S. Ponniah. 1997. Autoimmune prostatitis: evidence of T cell reactivity with normal prostatic proteins. *Urology* 50: 893–899.
7. Batstone, G. R., A. Doble, and J. S. Gaston. 2002. Autoimmune T cell responses to seminal plasma in chronic pelvic pain syndrome (CPPS). *Clin. Exp. Immunol.* 128: 302–307.
8. Hou, Y., J. DeVoss, V. Dao, S. Kwek, J. P. Simko, D. G. McNeel, M. S. Anderson, and L. Fong. 2009. An aberrant prostate antigen-specific immune response causes prostatitis in mice and is associated with chronic prostatitis in humans. *J. Clin. Invest.* 119: 2031–2041.
9. Alexander, R. B., S. Ponniah, J. Hasday, and J. R. Hebel. 1998. Elevated levels of proinflammatory cytokines in the semen of patients with chronic prostatitis/chronic pelvic pain syndrome. *Urology* 52: 744–749.

10. Nadler, R. B., A. E. Koch, E. A. Calhoun, P. L. Campbell, D. L. Pruden, C. L. Bennett, P. R. Yarnold, and A. J. Schaeffer. 2000. IL-1beta and TNF-alpha in prostatic secretions are indicators in the evaluation of men with chronic prostatitis. *J. Urol.* 164: 214–218.
11. Motrich, R. D., M. Maccioni, R. Molina, A. Tissera, J. Olmedo, C. M. Riera, and V. E. Rivero. 2005. Reduced semen quality in chronic prostatitis patients that have cellular autoimmune response to prostate antigens. *Hum. Reprod.* 20: 2567–2572.
12. John, H., A. Barghorn, G. Funke, T. Sulser, S. Hailemariam, D. Hauri, and H. Joller-Jemelka. 2001. Noninflammatory chronic pelvic pain syndrome: immunological study in blood, ejaculate and prostate tissue. *Eur. Urol.* 39: 72–78.
13. Motrich, R. D., M. Maccioni, C. M. Riera, and V. E. Rivero. 2007. Autoimmune prostatitis: state of the art. *Scand. J. Immunol.* 66: 217–227.
14. Rivero, V. E., C. Cailleau, M. Depiante-Depaoli, C. M. Riera, and C. Carnaud. 1998. Non-obese diabetic (NOD) mice are genetically susceptible to experimental autoimmune prostatitis (EAP). *J. Autoimmun.* 11: 603–610.
15. Motrich, R. D., M. Maccioni, A. A. Ponce, G. A. Gatti, J. P. Oberti, and V. E. Rivero. 2006. Pathogenic consequences in semen quality of an autoimmune response against the prostate gland: from animal models to human disease. *J. Immunol.* 177: 957–967.
16. Rudick, C. N., A. J. Schaeffer, and P. Thumbikat. 2008. Experimental autoimmune prostatitis induces chronic pelvic pain. *Am. J. Physiol. Regul. Integr. Comp. Physiol.* 294: R1268–R1275.
17. Keetch, D. W., P. Humphrey, and T. L. Ratliff. 1994. Development of a mouse model for nonbacterial prostatitis. *J. Urol.* 152: 247–250.
18. Penna, G., S. Amuchastegui, C. Cossetti, F. Aquilano, R. Mariani, N. Giarratana, E. De Carli, B. Fibbi, and L. Adorini. 2007. Spontaneous and prostatic steroid binding protein peptide-induced autoimmune prostatitis in the nonobese diabetic mouse. *J. Immunol.* 179: 1559–1567.
19. Motrich, R. D., E. van Etten, F. Baeke, C. M. Riera, C. Mathieu, and V. E. Rivero. 2010. Crucial role of interferon-γ in experimental autoimmune prostatitis. *J. Urol.* 183: 1213–1220.
20. Peters, A., Y. Lee, and V. K. Kuchroo. 2011. The many faces of Th17 cells. *Curr. Opin. Immunol.* 23: 702–706.
21. Ward, S. G., and F. M. Marelli-Berg. 2009. Mechanisms of chemokine and antigen-dependent T-lymphocyte navigation. *Biochem. J.* 418: 13–27.
22. Kunkel, E. J., and E. C. Butcher. 2002. Chemokines and the tissue-specific migration of lymphocytes. *Immunity* 16: 1–4.
23. Bono, M. R., R. Elgueta, D. Sauma, K. Pino, F. Osorio, P. Michea, A. Fierro, and M. Rosemblatt. 2007. The essential role of chemokines in the selective regulation of lymphocyte homing. *Cytokine Growth Factor Rev.* 18: 33–43.
24. McGeachy, M. J., K. S. Bak-Jensen, Y. Chen, C. M. Tato, W. Blumenschein, T. McClanahan, and D. J. Cua. 2007. TGF-beta and IL-6 drive the production of IL-17 and IL-10 by T cells and restrain T(H)-17 cell-mediated pathology. *Nat. Immunol.* 8: 1390–1397.
25. Ni, J., Y. N. Zhu, X. G. Zhong, Y. Ding, L. F. Hou, X. K. Tong, W. Tang, S. Ono, Y. F. Yang, and J. P. Zuo. 2009. The chemokine receptor antagonist, TAK-779, decreased experimental autoimmune encephalomyelitis by reducing inflammatory cell migration into the central nervous system, without affecting T cell function. *Br. J. Pharmacol.* 158: 2046–2056.
26. Suzaki, Y., K. Hamada, T. Nomi, T. Ito, M. Sho, Y. Kai, Y. Nakajima, and H. Kimura. 2008. A small-molecule compound targeting CCR5 and CXCR3 prevents airway hyperresponsiveness and inflammation. *Eur. Respir. J.* 31: 783–789.
27. Sallusto, F., and A. Lanzavecchia. 2009. Heterogeneity of CD4+ memory T cells: functional modules for tailored immunity. *Eur. J. Immunol.* 39: 2076–2082.
28. Cox, C. A., G. Shi, H. Yin, B. P. Vistica, E. F. Wawrousek, C. C. Chan, and I. Gery. 2008. Both Th1 and Th17 are immunopathogenic but differ in other key biological activities. *J. Immunol.* 180: 7414–7422.
29. Emamaullee, J. A., J. Davis, S. Merani, C. Toso, J. F. Elliott, A. Thiesen, and A. M. Shapiro. 2009. Inhibition of Th17 cells regulates autoimmune diabetes in NOD mice. *Diabetes* 58: 1302–1311.
30. Bending, D., H. De la Peña, M. Veldhoen, J. M. Phillips, C. Uyttenhove, B. Stockinger, and A. Cooke. 2009. Highly purified Th17 cells from BDC2.5NOD mice convert into Th1-like cells in NOD/SCID recipient mice. *J. Clin. Invest.* 119: 565–572.
31. Jankovic, D., and G. Trinchieri. 2007. IL-10 or not IL-10: that is the question. *Nat. Immunol.* 8: 1281–1283.
32. Martin-Orozco, N., Y. Chung, S. H. Chang, Y. H. Wang, and C. Dong. 2009. Th17 cells promote pancreatic inflammation but only induce diabetes efficiently in lymphopenic hosts after conversion into Th1 cells. *Eur. J. Immunol.* 39: 216–224.
33. Lau, K., P. Benitez, A. Ardissone, T. D. Wilson, E. L. Collins, G. Lorca, N. Li, D. Sankar, C. Wasserfall, J. Neu, et al. 2011. Inhibition of type 1 diabetes correlated to a *Lactobacillus* johnsonii N6.2-mediated Th17 bias. *J. Immunol.* 186: 3538–3546.
34. Nikoopour, E., J. A. Schwartz, K. Huszarik, C. Sandrock, O. Krougly, E. Lee-Chan, and B. Singh. 2010. Th17 polarized cells from nonobese diabetic mice following mycobacterial adjuvant immunotherapy delay type 1 diabetes. *J. Immunol.* 184: 4779–4788.
35. Tse, H. M., T. C. Thayer, C. Steele, C. M. Cuda, L. Morel, J. D. Piganelli, and C. E. Mathews. 2010. NADPH oxidase deficiency regulates Th lineage commitment and modulates autoimmunity. *J. Immunol.* 185: 5247–5258.
36. Joseph, J., S. Bittner, F. M. Kaiser, H. Wiendl, and S. Kissler. 2012. IL-17 silencing does not protect nonobese diabetic mice from autoimmune diabetes. *J. Immunol.* 188: 216–221.
37. Kriegel, M. A., E. Sefik, J. A. Hill, H. J. Wu, C. Benoist, and D. Mathis. 2011. Naturally transmitted segmented filamentous bacteria segregate with diabetes protection in nonobese diabetic mice. *Proc. Natl. Acad. Sci. USA* 108: 11548–11553.
38. O'Connor, W., Jr., M. Kamanaka, C. J. Booth, T. Town, S. Nakae, Y. Iwakura, J. K. Kolls, and R. A. Flavell. 2009. A protective function for interleukin 17A in T cell-mediated intestinal inflammation. *Nat. Immunol.* 10: 603–609.
39. Liu, M., S. Guo, J. M. Hibbert, V. Jain, N. Singh, N. O. Wilson, and J. K. Stiles. 2011. CXCL10/IP-10 in infectious diseases pathogenesis and potential therapeutic implications. *Cytokine Growth Factor Rev.* 22: 121–130.
40. Wang, C., S. G. Kang, J. Lee, Z. Sun, and C. H. Kim. 2009. The roles of CCR6 in migration of Th17 cells and regulation of effector T-cell balance in the gut. *Mucosal Immunol.* 2: 173–183.
41. Sallusto, F., D. Impellizzieri, C. Basso, A. Laroni, A. Uccelli, A. Lanzavecchia, and B. Engelhardt. 2012. T-cell trafficking in the central nervous system. *Immunol. Rev.* 248: 216–227.
42. Reboldi, A., C. Coisne, D. Baumjohann, F. Benvenuto, D. Bottinelli, S. Lira, A. Uccelli, A. Lanzavecchia, B. Engelhardt, and F. Sallusto. 2009. C-C chemokine receptor 6-regulated entry of TH-17 cells into the CNS through the choroid plexus is required for the initiation of EAE. *Nat. Immunol.* 10: 514–523.
43. Macoska, J. A. 2011. Chemokines and BPH/LUTS. *Differentiation* 82: 253–260.
44. Liu, L., Q. Li, P. Han, X. Li, H. Zeng, Y. Zhu, and Q. Wei. 2009. Evaluation of interleukin-8 in expressed prostatic secretion as a reliable biomarker of inflammation in benign prostatic hyperplasia. *Urology* 74: 340–344.
45. Desireddi, N. V., P. L. Campbell, J. A. Stern, R. Sobkoviak, S. Chuai, S. Shahrara, P. Thumbikat, R. M. Pope, J. R. Landis, A. E. Koch, and A. J. Schaeffer. 2008. Monocyte chemoattractant protein-1 and macrophage inflammatory protein-1alpha as possible biomarkers for the chronic pelvic pain syndrome. *J. Urol.* 179: 1857–1861, discussion 1861–1862.
46. Quick, M. L., S. Mukherjee, C. N. Rudick, J. D. Done, A. J. Schaeffer, and P. Thumbikat. 2012. CCL2 and CCL3 are essential mediators of pelvic pain in experimental autoimmune prostatitis. *Am. J. Physiol. Regul. Integr. Comp. Physiol.* 303: R580–R589.

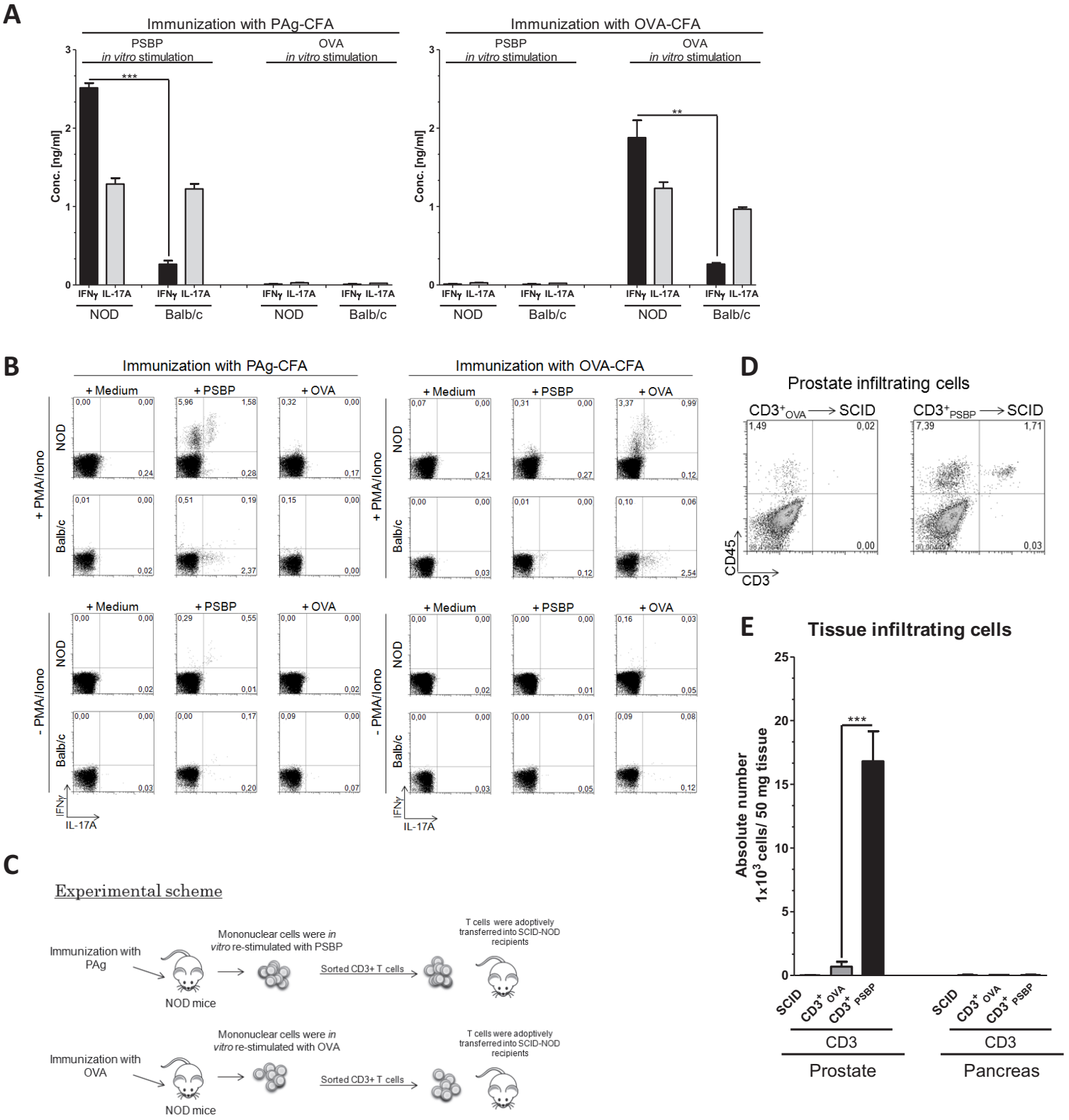

Supplemental Figure 1. Antigen specificity in PAg immunized mice. NOD and Balb/c mice were immunized with PAg or OVA emulsified CFA and euthanized at day 24. **A,** Levels of IFNγ and IL-17 in supernatants from spleen mononuclear cells stimulated *in vitro* with PSBP or OVA for 72 h (ELISA). Data are shown as mean ± SEM, n=5 per group, representative of two independent experiments. **B,** Representative intracellular staining for IFNγ and IL-17A was performed on spleen mononuclear cells after *in vitro* stimulation with PSBP or OVA for 72 h. Shown data were cells gated in the $CD4^+$ cell population. The cells were incubated with or without PMA/Ionomycin in presence of Brefeldin A for 5 hours. **C,** Experimental scheme for transfer experiments. **D,** Flow cytometry analysis of prostate tissue from recipients transferred with T cells from PAg or OVA immunized NOD mice. Mononuclear cells isolated from the prostate gland were counted excluding dead cells and then stained for CD45 and CD3; **E,** Absolute number of $CD3^+$ in the prostate and pancreas from NOD-SCID recipients at day 30 post-transfer. Data are shown as mean ± SEM, n=4 per group and are representative of two independent experiments. Statistical analyses were performed using one-way ANOVA

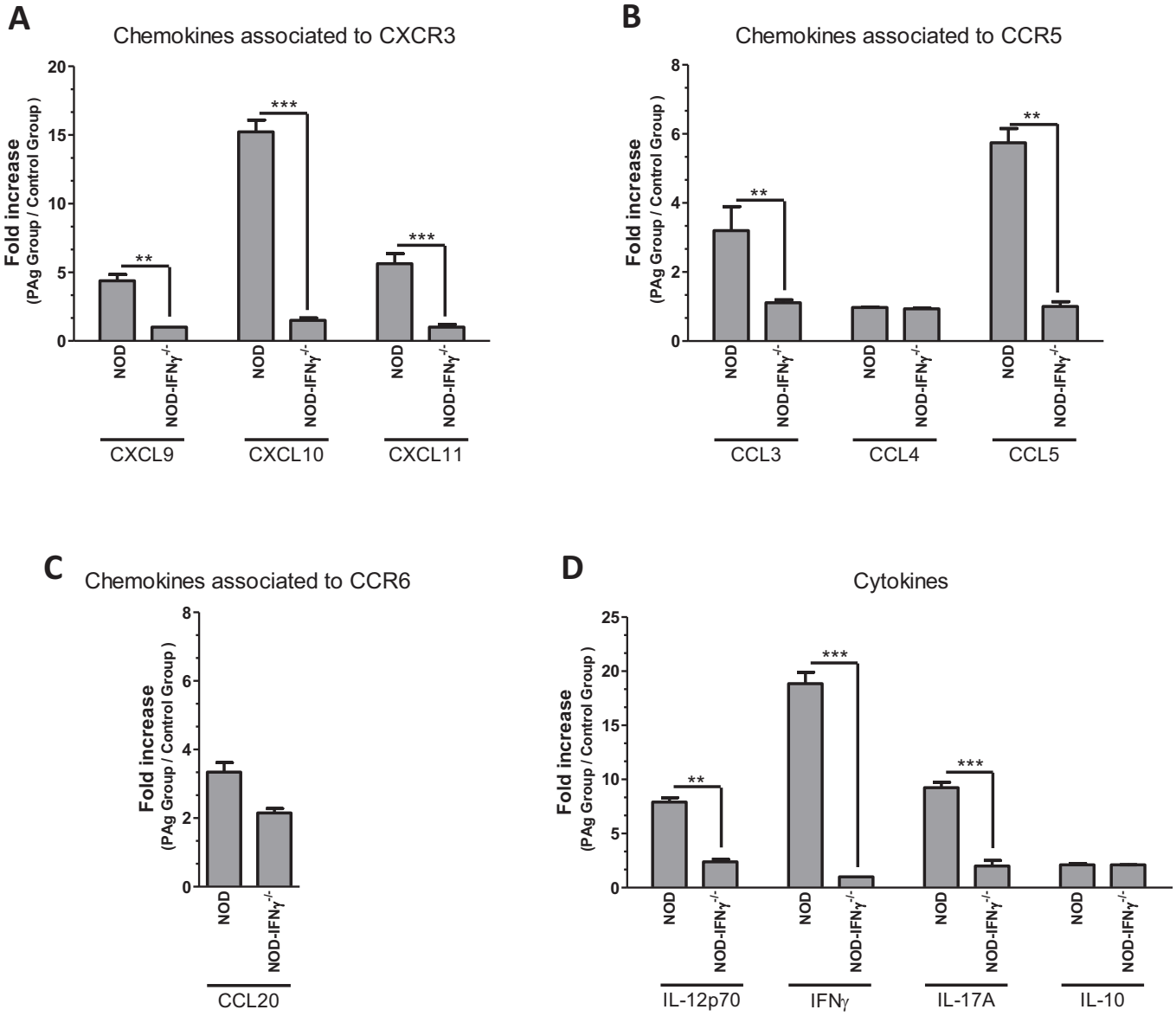

Supplemental Figure 2. Protein expression levels of chemokines and cytokines in prostate tissue from PAg immunized mice compared with the expression levels in control groups. **A** Fold increase in chemokines associated to CXCR3 receptor; **B** Fold increase in chemokines associated to CCR5 receptor; **C** Fold increase in chemokine associated to CCR6 receptor; **D** Fold increase in cytokines expressed in the prostate gland. Statistical analyses were performed using one-way ANOVA.

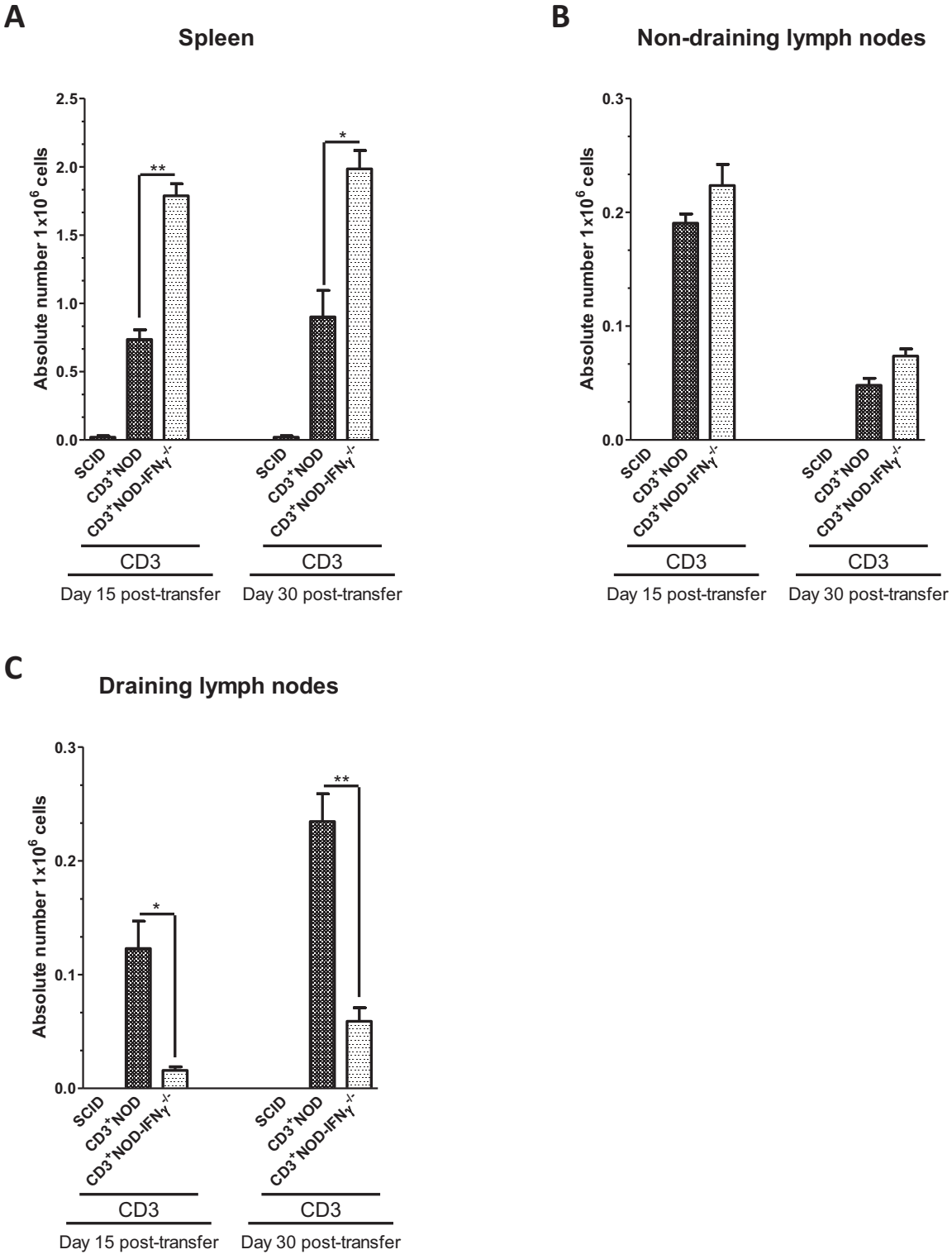

Supplemental Figure 3. Circulation of $CD3^+$ T cells from NOD and NOD-IFN$\gamma^{-/-}$mice in NOD-SCID recipient mice 15 or 30 days post adoptive transfer. **A,** Absolute number of $CD3^+$ T cells in spleen samples from NOD-SCID recipients at days 15 and 30 post-transfer; **B,** Absolute number of $CD3^+$ T cells in prostate non-draining lymph nodes from recipients; **C,** Absolute number of $CD3^+$ T cells in prostate draining lymph nodes from recipients. Data are shown as mean ± SD, n=2 recipients mice per group and are representative of three independent experiments. Statistical analyses were performed using one-way ANOVA.